Norwegian University
of Life Sciences

Master's Thesis 2021 30 ECTS
Faculty of Environmental Sciences and Natural Resource Management (MINA)

Effects of Stand Structure and Stand Density on Volume Growth and Ingrowth in Selectively Cut Stands in Norway

Maria Åsnes Moan
MSC Forest Science

Acknowledgements

I would like to thank my supervisor Professor Andreas Brunner for taking such a keen interest in my thesis, and for helping me whenever I needed it. I have learned a lot. I would also like to thank my co-supervisor Dr. Kjersti Holt Hanssen for valuable feedback and help with finding material for my thesis. Much needed help was received from PhD student Silke Houtmeyers with R-programming. I am also grateful for the funding I received from Universitetet for miljø- og biovitenskaps forskningsfond which made it possible to complete the fieldwork. A big thank you goes to Sverre Holm and Gunnar Aakrann Eek from Glommen Mjøsen Skog who helped coordinate the fieldwork and offered accommodation close to the KONTUS plots. I would like to thank the forest owners of the KONTUS plots for being helpful and having such a positive attitude.

I could not have completed this thesis nearly as well without my flatmates, who not only helped me understand mathematical concepts, but also offered much needed socialisation and emotional support in an isolated student life because of the Covid-19 pandemic. Last but not least, I would like to thank my mother for helping me think strategically about how to prioritize the work, and my father for revising the text.

Abstract

This thesis studied the effect of stand density on ingrowth, mortality, and volume increment in selectively cut stands in Norway. The effects of stand structure on growth were also addressed by determining the size-growth relationships.

Data was gathered from two experimental series in selectively cut stands in Norway. The main tree species was Norway spruce, except for one Scots pine site. Linear and non-linear regression models were used to study the effect of stand density (volume) on ingrowth, mortality, gross volume increment (*GVI*), and net volume increment (NVI).

The data showed that stand density did not have a significant effect on ingrowth or mortality. Most plots had concave size-growth relationships, meaning that trees with the smallest volumes contributed more to the volume increment relative to their size than trees with higher volumes. The models for *GVI* and *NVI* had an asymptotic shape for volume increment over stand density. These results were contrary to most other studies of the growth-density relationship in selectively cut stands. The size-growth relationship expressed as the Gini index did not explain any variation in volume increment, although the variation in Gini indices was large between plots.

The *GVI* model predicted volume increments at optimal density that were similar to the mean *MAI* from growth models for even-aged stands, illustrating how taking the stand density into consideration is imperative when comparing forest management systems.

Sammendrag

I denne oppgaven, ble det sett på hvordan bestandstetthet påvirker innvekst, mortalitet og volumtilvekst i selektivt hogde bestand i Norge. Effekten av bestandsstruktur på vekst ble også studert ved bestemmelse av såkalte «size-growth relationships».

Det ble hentet inn data fra to forsøksserier i selektivt hogde bestand i Norge. Hovedtreslaget var gran, foruten en lokalitet der hovedtreslaget var furu. Både lineære og ikke-lineære modeller ble brukt til å undersøke effekten av bestandstetthet på innvekst, mortalitet, brutto volumtilvekst, og netto volumtilvekst.

Det var ingen signifikant effekt av tetthet på innvekst eller på mortalitet. De fleste flatene hadde konkave «size-growth relationships», som vil si at de trærne som hadde minst volum bidro mer til den totale volumtilveksten i forhold til størrelsen enn de trærne med større volum. Modellene for brutto- og netto volumtilvekst predikerte at forholdet mellom brutto/ netto volumtilvekst og volum fulgte en asymtotisk kurve. Disse resultatene sto i kontrast til tidligere studier i selektivt hogd skog. Gini indeks, som ble beregnet som uttrykk for «size-

growth relationship», forklarte ikke noe variasjon i volumtilvekst selv om flatene hadde svært ulike Gini indekser.

Modellen for brutto volumtilvekst predikerte volumtilvekst ved optimal tetthet som sammenfalte godt med gjennomsnittlig årlig middeltilvekst beregnet for ensjiktede bestand. Dette illustrerer hvor viktig det er å ta bestandstetthet med i beregningen når vi sammenligner skogskjøtselssystemer.

Table of Contents

Introduction

Continuous cover forestry (CCF) has gained interest in Norway and other Nordic countries in the last decades, because of increased focus on forests as providers of multiple ecosystem services. CCF is characterised by maintaining a permanent forest cover and that "management is based on the selection and favouring of individual trees" (Helliwell & Wilson, 2012). Pukkala (2016) found that stands managed by CCF might provide more ecosystem services than even-aged stands. Biodiversity and recreation are two ecosystem services where the application of CCF might be beneficial. Savilaakso et al. (2021) reviewed 137 articles with 854 studies in Fennoscandia and European Russia and found that uneven-aged forest management hosted more forest dependent species than even-aged forests with a stand age below 80 years. Lindhagen and Hörnsten (2000) found that virgin forests received higher scores in questionnaires about recreational preferences in Sweden in 1997 compared to 1977, while even-aged forests decreased in popularity between the two time periods. With increasing popularity of CCF, there is a need for more knowledge about the management of forests where CCF is applied.

Terminology

The selection system is a silvicultural system that can be applied to reach the goals of CCF. In the selection system, the aim is to keep a stand with a falling diameter distribution and trees of all heights. In harvests, single trees are removed, but the structure of the stand remains intact. The selection system usually relies on natural regeneration, but it is also a possibility to plant trees within stands that are managed by the selection system. (Lundqvist et al., 2014). There are several silvicultural methods that can be applied within the selection system. For instance, there is the silvicultural method of target diameter cutting, which is also called diameter limit harvest, that involves harvesting trees above a certain diameter at breast height (*DBH*) (Sterba & Zingg, 2001).

The selection system is said to be best suited in stands with a falling diameter distribution. This is because the falling diameter distribution can remain stable over time even though individual trees are harvested at set harvesting intervals (Sterba, 2004). Still, one important consideration is that there needs to be enough new trees to replace trees that are harvested and trees that die naturally (Lundqvist et al., 2014), if the stand structure in selectively cut stands is to remain stable over time. The optimal shape of this distribution has been proposed by several studies (De Liocourt 1898, cited in Sterba 2004; Schütz 1975, cited in Sterba 2004). De Liocourt observed uneven-aged forests in France and described the distribution mathematically as a negative exponential function or an inversed J-shape. In the inversed J-shape proposed by De Liocourt, the ratio between two neighbouring diameter classes is called *q* and this ratio remains constant throughout the diameter distribution. Schütz claimed that if there was as many trees growing into a diameter class as there were trees growing out of the same diameter class or being harvested/dying, the diameter distribution would remain stable (De Liocourt 1898, cited in Sterba 2004; Schütz 1975, cited in Sterba 2004). Ahlström and Lundqvist (2015) proposed a new term, "full-storied". The diameter distribution was divided

into four parts: D1, D2, D3 and D4. A forest is said to be “full-storied” when there were more trees in D1 than in D2, and D2 contained more trees than D3, and so on. Uneven-aged, uneven-sized, multi-layered, all-sized, etc. are broader terms which are used to describe forests which deviate from the single-storied structure (Lundqvist, 2017). I will use the term “selectively cut” when writing about the harvesting of these forests, and the term “selection system” when referring to the management system itself. I might also use the term “uneven-aged” when the focus is on the structure of the forests managed by the selection system.

Stand density and ingrowth

In the selection system, there is usually no planting after harvest, and it is important to have sufficient natural regeneration to ensure the sustainability of the forest management system. In the beginning of the regeneration process there are many things that can go wrong and subsequently there is high mortality among the smallest trees (Smith et al., 1997). In research plots, small trees are often first registered when they have grown into the tree stratum and become ingrowth trees. “Ingrowth is defined as the process whereby small trees grow past a certain size threshold into the tree stratum” (Lundqvist, 2017). This threshold has varied considerably between studies, with a *DBH* of 5-8 cm being the most common thresholds (Lundqvist, 2017). The growth of small trees in selectively cut forests is slow in the beginning and seems to be increasing with increasing size of the trees. A spruce seedling might use 60 years to reach breast height and an additional 20–50 years to reach a *DBH* of 5 cm (Eerikäinen et al., 2014). So, it might take almost a century for a sapling to become an ingrowth tree (Lundqvist, 2017).

Studying the relationship between density and ingrowth is an important contribution to the balance between high density to increase volume growth and low density to enable ingrowth. The studies cited below are all from spruce sites in uneven-aged forests. The number of trees growing past 1.3 meters height was 30.4 trees ha^{-1} $year^{-1}$ in a study in Southern Finland with stand densities in terms of volume in the range 91 to 371.3 m^3 ha^{-1} (Eerikäinen et al., 2014). Lundqvist et al. (2007) studied ingrowth in two field experiments in spruce forest in Central and Northern Sweden. The densities expressed as volume ranged from 18 to 289 m^3 ha^{-1} at the site in Central Sweden and from 19 to 238 m^3 ha^{-1} at the site in Northern Sweden. The number of ingrowth trees past a threshold of 5 cm in *DBH* at unthinned plots was on average 12 trees ha^{-1} $year^{-1}$ at the site in Central Sweden and 7 trees ha^{-1} $year^{-1}$ at the northern site. There was a significant negative effect ($p < 0.001$) of stand density on ingrowth in the plot in central Sweden, but a nonsignificant negative effect for the plot in northern Sweden (Lundqvist et al., 2007). Ahlström and Lundqvist (2015) studied stands where the density was heavily reduced after harvest for all plots. Densities before harvests ranged from 94 to 227 m^3 ha^{-1}, while after harvest they ranged from 34 to 88 m^3 ha^{-1}. The average number of ingrowth trees ranged from 8.1 to 21.7 trees per ha. The ingrowth was higher at higher stand volumes, but this correlation was insignificant and probably caused by some of the harvests which increased height growth and not the density of the ingrowth (Ahlström & Lundqvist, 2015). Height growth of small trees has an effect on the number of ingrowth trees because it influences how fast small trees grow into the tree stratum and become ingrowth. Chrimes and Nilson (2005) found that height growth was negatively, but insignificantly correlated with volume and basal area. Lundqvist

(2004) studied uneven-aged forests in sub-alpine areas with densities after harvest between 9-37 m^3 ha^{-1} and did not find a negative effect of stand volume after harvest on ingrowth. The results vary, but most studies did not find any effect, or only a small negative effect, of stand density on ingrowth.

Stand structure and volume increment

The selection system is often applied in stands with a falling diameter distribution, in other words, in stands with high structural diversity. A way to quantify structural diversity for a given variable, e.g basal area or height, is by calculating the Gini index, where a higher Gini index means that there is more structural diversity (Lei et al., 2009). Whether this structural diversity is positive or negative for growth is important for determining the productivity of forests managed by the selection system. Lei et al. (2009) studied forests dominated by spruce species in Canada and found that Gini index describing the structural diversity in basal area, did not significantly affect volume growth. Bourdier et al. (2016) found no effect of differences in Gini index calculated for basal area on basal area growth per year in Norway spruce stands in France. For many other tree species, there was a significant negative effect in the same study. Bianchi et al. (2020) developed growth models with data from Norway spruce-dominated stands in Southern Finland, which had been managed with single-tree selection, and found that a higher Gini index for height, had a small, but significant effect on the stand growth.

Forrester (2019) reviewed how stand structure might affect stand growth, by using a conceptual framework with three factors: stand density, stand structure, and the tree size-growth relationship. The tree size-growth relationship describes how the trees in a stand grow relative to their size. It is emphasised that if this framework is to be used, all these factors need to be in the same unit. If volume (m^3) is chosen as the unit, the stand density must be expressed as the volume in m^3 ha^{-1}. It follows that the stand structure must be expressed as the amount of volume (m^3) or relative volume (%) in different diameter classes, and the size-growth relationship expressed as the volume increment (m^3 ha^{-1} $year^{-1}$) of trees of different sizes (Figure 1). If the relative cumulative volume increment is plotted against the relative cumulative volume, the tree size-growth relationship and the stand structure can be analysed together, and this is the size-growth relationship.

The size-growth relationship is the relationship between the cumulative relative increment and the cumulative relative density in a stand, if trees are sorted according to their size. If all trees grow proportional to their size, the size-growth relationship will follow the 1:1-line meaning that there will be one increase in relative increment for one increase in relative tree volume. If smaller trees grow more in proportion to their size than larger trees in the same stand, the relationship will be concave. If the larger trees grow more in proportion to their size than smaller trees in the same stand, the relationship will be convex. Concave means that the curve is above the 1:1-line and convex means that the curve is below the 1:1-line. Both the stand structure and the growth of individual trees relative to their size will influence the size-growth relationship. If, for instance, there are many smaller trees in the stand and the smaller trees grow the most in proportion to their size, then there will be a concave relationship (Figure 1

a). If, on the other hand, there are many small trees in the stand, but the largest trees grow the most in proportion to their size, then the relationship will be convex (Figure 1 b). If the size-growth relationship is the same as the examples above, but the size-distribution shifts and becomes bell-shaped, then there will still be a concave and a convex curve like before, but these curves will differ less from the 1:1-line (Figure 1 c and d). The Gini index calculated for the size-growth relationships is another way of displaying the size-growth relationships and comparing them.

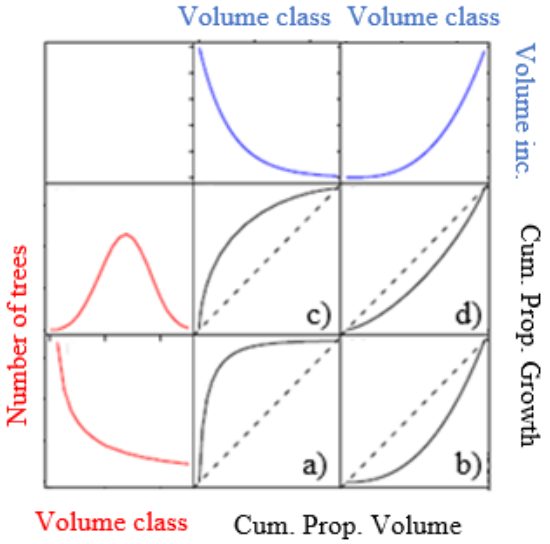

Figure 1: Example of four different size-growth relationships (a-d). Red lines are frequency distributions, showing the number of trees in different size classes. Blue lines are the growth of trees of different size. The blue line on the left indicates that smaller trees grow the most relative to their size and the blue line on the right indicate that larger trees grow the most relative to their size. This figure is based on Fig. 1 in Forrester (2019).

Few studies have looked at the size-growth relationship of stands where there have been selective cuttings. Andersson (2015) studied the size-growth relationship of plots of spruce and pine managed with selective cutting, The KONTUS plots, in 2015, and found concave size-growth relationships in four of six plots. Castagneri et al. (2012) found that a multi-layered spruce plot managed with selective cutting in the north-east of Italy had a concave size-growth relationship, meaning that the small trees grew more in relation to their size than the larger trees.

It is unclear whether a concave size-growth relationship has a positive or negative effect on stand growth. Forrester (2019) claims that if resource partitioning changes in favour of size classes with an abundance of trees, then that is positive for stand growth.

Stand density and volume increment

The relationship between stand volume increment and stand density, the growth-density relationship, is important in stands managed by the selection system. Harvesting reduces the stand density, and it is usually desirable to keep a stand density that gives a large volume increment. It is therefore important to know how density affects volume increment to plan the harvesting regime in selectively cut forests. When studying the relationship between volume increment and stand density, studies of even-aged stands have used several measures of density such as the number of trees, basal area, or volume (Zeide, 2001). In studies of uneven-aged stands, stand volume is mostly used as the measure for stand density. This is because uneven-aged stands are characterized by large variations of heights (Lundqvist, 2012), which means that there is a need to use a variable that is sensitive to this variation.

Stand volume increment might be defined in several ways. An important distinction is between gross volume increment (*GVI*) and net volume increment (NVI), which are calculated based on the gross volume and the net volume. The gross volume is the volume of all trees, i.e., the volume of standing, harvested, and dead trees. The net volume is the volume of standing trees and harvested trees only (Avery & Burkhart 2015, cited in Allen et al. 2020). *GVI* is the change in gross volume and *NVI* is the change in net volume.

Differences between *NVI* and *GVI* are caused by mortality. In uneven-aged stands, mortality has been assumed to be low (Valkonen et al., 2020). Valkonen et al. (2020) tested whether mortality increased with increasing stand density in managed uneven-aged spruce stands in Southern Finland. The number of trees (trees ha^{-1}), basal area (m^2 ha^{-1}), and volume (m^3 ha^{-1}) were used as the measures for density and the mortality had the same unit as the measure of density which it was compared to. An increasing relationship was found when plotting the data, but the relationships were not significant. This was just one study, and conclusions about the relationship between mortality and density in selectively cut forests cannot be made only based on this.

Many studies of selectively cut stands have concluded that volume increment increases with increasing stand density (Ahlström & Lundqvist, 2015; Lundqvist et al., 2007; Lähde et al., 1994; Lähde et al., 2002; Näslund, 1942), while a few studies did not find a significant relationship (Valkonen et al., 2017; Øyen & Nilsen, 2002). Some studies have also sought to quantify the relationship between stand density and volume increment, i.e., determining the shape of the curve. Chrimes (2004) modelled volume increment depending on volume for managed uneven-aged spruce stands with densities in the range 99-256 m^3 ha^{-1}. He found that if trees were harvested by diameter-limit harvest, the non-linear relationship reached the optimum at 197 m^3 ha^{-1} and then declined. The author pointed out that even though one would expect mortality to cause lower volume increment at higher volumes, mortality was not included in the model. It was suggested that the decrease after the optimum might be influenced by the formulation of competition variables and the fact that there was very little data above 200 m^3 ha^{-1}. Lundqvist (2012) combined data from table 27 and figure 47 in Näslund (1942) which enabled him to find the increment in m^3 ha^{-1} $year^{-1}$ after thinning for stands with different densities (volume) and site fertilities. The site fertility was quantified by the vegetation type at the site, and the maximum density was 324.5 m^3 ha^{-1} for the more fertile site in the comparison and 215.0 m^3 ha^{-1} for the less fertile site (Näslund, 1942). The

relationship was degressive, which means that it increased with increasing volume and the slope of the curve became less steep as volume increased. For the less fertile vegetation type, the curve reached an optimum at around 250 m^3 ha^{-1} which was outside the range of the data, while for the more fertile vegetation type, no optimum was reached. Näslund's study was conducted in old spruce stands in northern Sweden. Results from selectively cut spruce forests in Southern Finland showed a degressive, but weak relationship between mean annual volume growth (m^3 ha^{-1}) and stand basal area (m^2 ha^{-1}) (Hynynen, 2014). The curve became flatter at around 20 m^2 ha^{-1} and there was no sign of an optimum at the highest density in the data, which was around 28 m^2 ha^{-1}.

According to Lundqvist (2017) one can expect either an asymptotic or optimum curve to describe the relationship between volume and volume increment and neither of these patterns have been found for uneven-aged stands. A possible explanation for this is that the forests have not reached a density where the volume increment is maximized in any of the studies (Lundqvist, 2017). In the selection system, it is necessary to keep a density that enables ingrowth. The ingrowth is low at very high stand densities and so the densities in studies of selectively cut forests are not very high. Because of this, the relationship between stand density and volume increment at higher densities is not yet known. Yet, the studies so far seem to be in support of a degressive relationship. Degressive means that the slope of the curve is decreasing. It differs from the asymptotic relationship since the slope will not be 0 and from the optimum relationship since the slope will not be negative.

For even-aged stands, the growth-density relationship has been studied more extensively. The growth-density relationships which were found in several earlier studies suggested an asymptotic curve (Allen et al., 2020). Assmann (1970, cited in Skovsgaard and Vanclay 2008) found an optimum curve which challenged the results of earlier studies. In studies of even-aged stands, the densities studied were much higher than for studies of uneven-aged stands. For instance, Allen et al. (2020) found an asymptotic shape for gross volume increment reaching the asymptote at a basal area of 62 m^2 ha^{-1} and an optimum curve for the net volume increment at 43 m^2 ha^{-1}.

Experiments on selective cutting in Norway

The KONTUS plots

The KONTUS project was established by the forest owner associations Glommen Skog and Mjøsen Skog. They wanted to develop and document methods of CCF and its consequences by testing a harvesting method called KONTUS on some selected sites. KONTUS was inspired by the method of "naturkultur" by Mats Hagner (Glommen Skogeierforening & Mjøsen Skogeierforening, 2005). The "naturkultur"-method was based on an economical criterion where trees should be harvested if their growth did not satisfy a certain rate of return (Hagner 2015, cited in Andersson 2015). In practice, the harvest resembled a target diameter cutting, since the approach led to almost only large trees being harvested, but this was not always the case, e.g., smaller trees with poor quality were harvested as well and dense groups of trees were thinned (Økseter & Myrbakken, 2005). The KONTUS project originally

included 15 sites in the Innlandet region (Glommen Skogeierforening & Mjøsen Skogeierforening, 2005), but today only seven sites remain intact. These seven sites were remeasured and analysed in the master thesis of Andersson (2015). He found that the plots had a stand volume ranging from 67.3 - 278.8 m^3 ha^{-1}. The periodical volume increment ranged from 3.1 - 5.6 m^3 ha^{-1} $year^{-1}$. Volume increment increased with increasing volume and discrepancies in this relationship were explained by differences in stand structure, more specifically by the size-growth relationship.

The selection system plots

The selection system experiment series were established between 1921 and 1939 by the Norwegian Forest Research Institute (Andreassen, 1994). Analyses of the data from those plots were done in the doctoral thesis of Peder Braathe in 1952, a study by Johan G. Böhmer published in 1957 (Woxholtt & Orlund, 2009), and a study by Kjell Andreassen published in 1994. Andreassen (1994) compared the volume increment in the selection system plots with the yield potential according to growth models for even-aged stands and concluded that the selection system plots produced on average 15-20% less volume than even-aged stands with the same site index. Andersson (2015) and Lundqvist (2012) have pointed out that volume increment increased with increasing volume in the data from this experimental series and that Andreassen (1994) did not account for this large effect of stand density in the analysis. After correcting for stand density, volume increment in the selection system plots was at a comparable level to that in growth models for fully stocked even-aged stands (Andersson, 2015). Today, the Norwegian Institute of Bioeconomy Research (NIBIO) oversees the selection system experiments, and some of them are still remeasured at regular intervals.

Objective of the study

The objective of this study is to use data from the two Norwegian experimental series in selectively cut stands, described above, to assess the relationship between stand volume increment and stand density and how stand structure affects this relationship. I also aim to look at how density affects ingrowth in these stands.

Based on the existing knowledge presented above, the following hypotheses have been derived:

1) Ingrowth decreases with increasing stand density.
2) The size-growth relationship is likely concave.
3) The relationship between stand density (expressed as stand volume) and stand volume increment (*GVI* and NVI) is degressive.

Material and methods

KONTUS plots

The seven sites which were part of the KONTUS project are located in the south-eastern part of Norway (Table 1). All sites were primarily dominated by spruce except for site 3, which was dominated by pine.

Table 1: Site characteristics for the KONTUS plots. Site index (m) for sites 1-3 are from Hanssen et al. (2007) while the site indices for sites 4-7 are from Glommen Skogeierforening and Mjøsen Skogeierforening (2005).

Site	Plot	Area (ha)	Elevation (m)	Site Index (m)	Longitude (degree)	Latitude (degree)	Municipality
1	1	0.2	450	G14	11°28'E	60°30'N	Nord-Odal
1	2	0.2	450	G14	11°28'E	60°30'N	Nord-Odal
2	1	0.2	540	G12	11°35'E	60°39'N	Stange
2	2	0.2	540	G12	11°35'E	60°39'N	Stange
3	1	0.2	520	F11	10°57'E	62°23'N	Tolga
3	2	0.2	520	F11	10°57'E	62°23'N	Tolga
4		0.1	500	G13	12°29’E	61°13’N	Trysil
5		0.1	510	G14	12°11’E	61°04’N	Trysil
6		0.1	290	G14	11°29’E	61°15’N	Åmot
7		0.1	390	G11	11°41’E	60°30’N	Nord-Odal

Treatments

Harvesting was done in all seven sites in the winter of 2003/2004 (Glommen Skogeierforening & Mjøsen Skogeierforening, 2005). Sites 1 - 3 were experiments by the Norwegian Institute of Bioeconomy Research (NIBIO) and their research design differed from sites 4 - 7. Each of the sites 1 – 3 consisted of two plots, which had been subject to different harvest intensities. In plot 1, 60% of the volume were to remain after harvest, while in plot 2, 40% were to remain (Hanssen, 2007). In reality, the difference in harvest intensity between plots was not as big as intended.

On sites 1-3, spruce and pine trees were planted in 2004 as part of a study on regeneration. Spruce and pine were planted interchangeably in rows, and coordinates were recorded for some of the planted trees (Aulie, 2013).

Measurements

The KONTUS plots on sites 1-3 were measured before and after the harvest in 2003/2004. In 2014, all 10 KONTUS plots on the seven sites were remeasured as a part of a master thesis (Andersson, 2015). In the context of this study, these 10 plots were remeasured over the course of three weeks in June 2020. A description of the measurements from 2020 is given below.

For all trees that had also been measured in 2014, diameter at breast height (*DBH*) and whether the tree was dead was recorded. *DBH* was measured with a diameter tape and measurement height was permanently marked on the trees during earlier measurements. For some trees, height (m) and the height to the crown base (m) was measured with a Vertex tree height measuring device. Trees that were registered as dead in 2014 were not remeasured in 2020. If a tree was damaged or had other noteworthy characteristics, this was recorded.

Trees that had grown past breast height since 2014, i.e. above 1.3 m, were recorded as ingrowth trees. This threshold was chosen for consistency with earlier measurements of ingrowth in these plots (Andersson, 2015). For the ingrowth trees, *DBH*, tree species, and position were recorded. The position was found by measuring the distance to the four closest neighbouring trees with known coordinates using a Vertex distance measurement device. The neighbouring trees had to be located evenly around the tree, i.e. not only on one side. After the field work, the four distances were used to estimate the coordinates of the ingrowth tree.

Selection system experiments

Originally, the selection system experiments consisted of 30 plots spread across Norway (Andreassen, 1994). Only data which was available digitally and had more than one measurement, was used in this study. Only 7 of the selection system plots met this requirement and, in these plots, only data from the last registrations were available digitally and could be used in this study (Table 4). These plots were located in the northern, central, and eastern parts of Norway (Table 2).

Table 2: Site characteristics for the selection system plots. Site index (m) is the mean of four different estimating techniques for site index (Andreassen, 1994). Plot 90 has an area of 1 ha, but only 0.6 ha of the plot had a satisfactory stand structure and was used in this study.

Plot	Area (ha)	Elevation (m)	Site Index (m)	Longitude (degree)	Latitude (degree)	Municipality
36	0.4	100	14.5	11.35	64.35	Namsos
61	0.948	200	13.6	12.70	65.50	Hattfjelldal
90	0.6	80	18.0	11.25	59.50	Indre Østfold
145	0.685	130	14.9	11.50	64.25	Namsos
178	0.635	50	11.9	12.40	65.85	Vefsn
329	1.24	800	11.0	10.60	61.70	Ringebu
453	0.515	200	15.1	12.40	64.60	Grong

Treatments

Since 1977, harvests had been done in plots 36, 61, and 90. In some cases, a few trees have been registered as harvested even though this was not in the context of a planned harvest. Table 3 gives the harvested volumes.

Table 3: Harvested volume in the selection system plots.

Plot	Year	Harvested volume (m^3 ha^{-1})
36	2015	22.0
61	2001	1.14
61	2013	5.68
90	2005	111
145	2015	0.176
329	2008	0.0115

Measurements

The selection system plots are measured by NIBIO periodically. Although these are long-term experimental plots with the first measurements between 1921 and 1939 (Andreassen, 1994), only measurements after 1977 were available for this study. In some contexts in this study, the number of the measurement or registration (first, second or third), will be used instead of the measurement year. Table 4 shows which years that correspond to each measurement.

Table 4: The measurement year for plots in the selection system experiments used in this study.

Plot	Registration number		
	1	2	3
36	1977	1990	2015
61	1990	2001	2013
90	2005	2020	-
145	1979	1990	2015
178	1990	2001	-
329	1989	2000	2008
453	1989	2000	-

Calculations

Data from the registrations in the KONTUS plots was added to an already existing dataset including measurements from 2004 and 2014. This dataset was the basis of all analyses of the data from the KONTUS plots. I used an existing dataset from NIBIO containing measurements from the selection system plots. The statistical software R was used for calculation and analysis of the data.

Height-diameter regression and volume calculation

Since height is needed to calculate volume, heights were estimated for all trees without a height measurement. Estimation of heights was done by determining the height-diameter relationships of trees with height measurements using non-linear regression. Height-diameter relationships are likely to vary between plots and species and might also vary between years as described by Sharma and Breidenbach (2015) and references therein.

The residual plots from the regression for the KONTUS plots suggested no bias or patterns in the residuals for data from different years (Figure 3), so measurements from all the years were pooled in the regression. Twelve regression models were developed for the KONTUS plots. For spruce, a model was developed for each plot, except for site 3 where a pooled model was used including both plot 1 and 2 because of few measurements of spruce on this site. Pine models were developed only for site 3 with separate models for plot 1 and 2. For broadleaved trees, all measurements across all sites were pooled and only one model was fitted.

The residual plots from the selection system plots showed a bias for data from different years. For spruce, regressions were fitted for each measurement year and plot. Regressions were fitted for broadleaved trees in plot 36, 90, 145, and 329. No plots had enough pine trees to do a regression for this species separately and some plots did not have enough broadleaves to do

a separate regression for broadleaved trees. In these plots, the regression of spruce trees was used to estimate tree heights for other species.

The response variable in the regression was *height* – 1.3 m since the model predicts better when the smallest heights are close to zero. A non-linear function (Equation 1) was used (Figure 2, Figure 3). In equation 1, *H* is height in meters, *DBH* is in cm, and *a*, *b*, and *c* are parameters which were estimated with the nls-function in R.

$$H\ -1{,}3\ m = a\ \times (1 - \exp(-b \times DBH))^{c} \qquad (1)$$

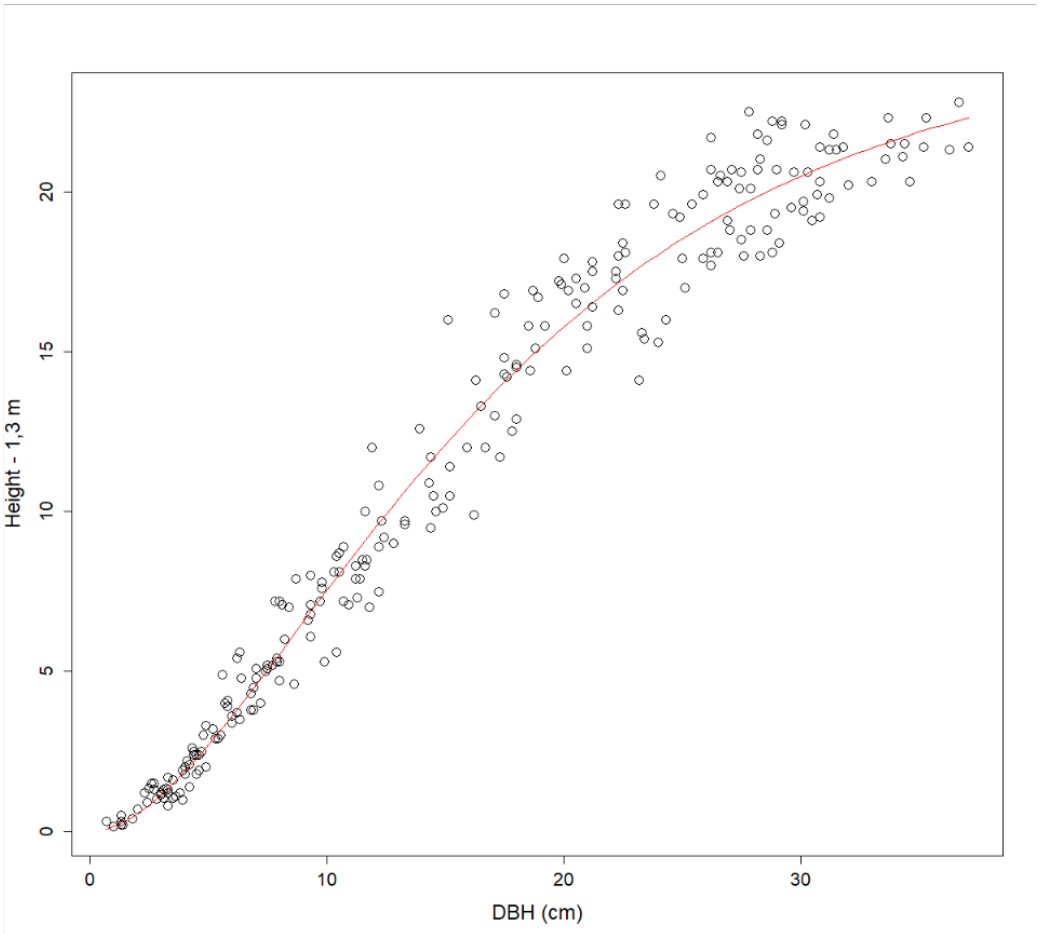

Figure 2: The fitted regression line (red line) for spruce trees in Site 1 plot 2. The empty circles are observed data.

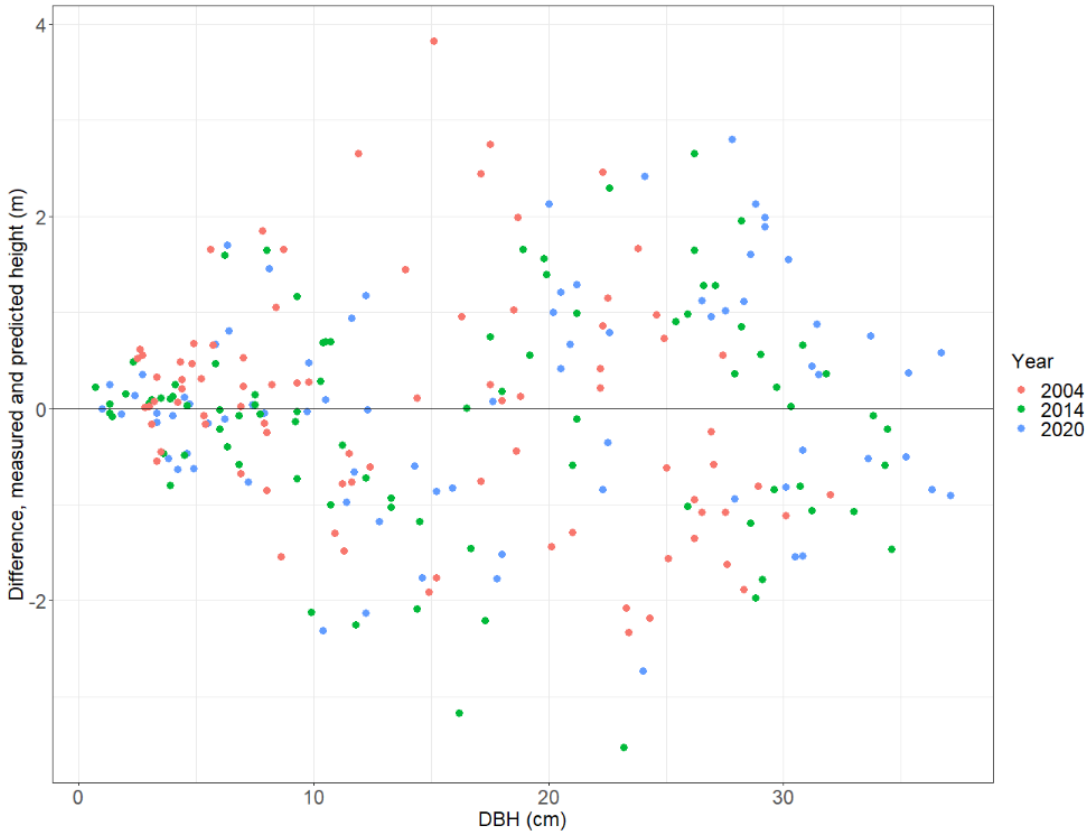

Figure 3: Plot of residuals of the heigh-diameter regression model for spruce trees in Site 1 plot 2.

Table 5 and 6 contain the parameter estimates and fit statistics for the regression models. An approximation of *RMSE* was calculated by taking the square root of *RSS* divided by the number of observations.

For estimating tree heights, 1.3 was added to the predictions of H – 1.3 m.

Table 5: Parameter estimates and fit statistics of the height-diameter regression models for the KONTUS plots. RSS is the Residual Sum of Squares. RMSE is the root mean square error.

Tree species	Site	Plot	Parameter estimates			Number of observations	*RSS*	*RMSE* (m)
			a	*b*	*c*			
Spruce	1	1	24.23	0.08316	2.113	150	219.5	1.21
		2	24.82	0.07944	1.986	252	330.8	1.15
	2	1	28.71	0.03698	1.304	141	155.6	1.05
		2	20.98	0.0797	1.882	232	281.5	1.10
	3	1 & 2	25.89	0.04505	1.344	31	5.6	0.42
	4		22.40	0.09623	2.089	42	103.7	1.57
	5		36.75	0.03844	1.493	41	89.7	1.48
	6		26.51	0.08106	1.870	43	103.8	1.55
	7		22.81	0.07946	1.727	43	30.1	0.84
Pine	3	1	19.88	0.1093	1.832	114	223.4	1.40
	3	2	15.88	0.1192	1.617	104	256.0	1.57
Broadleaved	All	All	22.09	0.08197	1.354	193	271.5	1.19

Table 6: Parameter estimates and fit statistics of the height-diameter regression models for the selection system plots.

Tree species	Plot	Year	Parameter estimates			Number of observations	*RSS*	*RMSE* (m)
			a	b	c			
Spruce	36	1977	26.4793	0.0481	1.3524	105	174	1.29
		1990	25.16509	0.06304	1.48557	176	244.9	1.18
		2015	25.71969	0.07703	1.71073	258	459.2	1.33
	61	1990	25.66728	0.06784	1.69765	307	624.6	1.43
		2001	26.24927	0.06674	1.68901	311	718.5	1.52
		2013	27.49650	0.06349	1.62146	322	907.2	1.68
	90	2005	33.29421	0.04533	1.33010	412	1974	2.19
		2020	31.10749	0.05935	1.62263	396	1401	1.88
	145	1979	28.69877	0.03865	1.28680	142	204	1.20
		1990	28.24440	0.04088	1.28128	205	262.6	1.13
		2015	27.18317	0.06611	1.61521	406	692.3	1.31
	178	1990	21.25793	0.08942	1.87015	265	362.2	1.17
		2001	21.55688	0.09431	2.10392	267	459.6	1.31
	329	1989	26.047	0.035	1.186	333	823.6	1.57
		2000	24.56104	0.03611	1.10984	301	680.3	1.50
		2008	23.68236	0.04366	1.18197	425	1081	1.59
	453	1989	27.33099	0.04717	1.33840	151	543.5	1.90
		2000	26.27497	0.05073	1.40415	162	664.5	2.03
Broadleaved	36	All	19.61104	0.08388	1.24960	44	86.46	1.40
	90	All	24.3646	0.0470	0.8008	82	253.2	1.76
	145	All	16.3662	0.1034	1.1381	101	110.3	1.05
	329	1989	64.507532	0.001528	0.534096	130	103.3	0.891
		2000	15.07726	0.04886	0.70993	119	126.8	1.03
		2008	13.1470	0.0817	0.7936	118	192.3	1.28

The volume of spruce trees were calculated using the volume functions developed by Vestjordet (1967). The volume calculated from equations 2-7 is stem volume with bark in dm^3. *H* is in m and *DBH* is in cm.

Spruce trees with a *DBH* less than 10 cm:

$$Volume = 0.52 + 0.02403 \times DBH^2 \times H + 0.01463 \times DBH \times H^2 \\ -0.10983 \times H^2 + 0.15195 \times DBH * H \quad (2)$$

Spruce trees with a *DBH* between 10 cm and 13 cm:

$$Volume = -31.57 + 0.0016 \times DBH \times H^2 + 0.0186 \times H^2 + 0.63 \times DBH \times H \\ -2.34 \times H + 3.20 \times DBH \quad (3)$$

Spruce trees with a *DBH* greater than 13 cm:

$$Volume = 10.14 + 0.01240 \times DBH^2 \times H + 0.03117 \times DBH \times H^2 \\ -0.36381 \times H^2 + 0.28578 \times DBH \times H \quad (4)$$

To calculate the volume of pine trees, the volume functions developed by Brantseg (1967) were used. Brantseg developed one function for pine trees with a *DBH* greater than 10 cm and another for pine trees with a *DBH* less than 12 cm. I used the function for smaller pine trees for all trees with a *DBH* less than or equal to 10, and the function for larger pine trees for all trees with a *DBH* greater than 10 cm.

Pine trees with a *DBH* less than or equal to 10 cm:

$$Volume = 2.0044 + 0.029886 \times DBH^2 + 0.036972 \times DBH^2 \times H \quad (5)$$

Pine trees with a *DBH* greater than 10 cm:

$$Volume = 8.6524 + 0.076844 \times DBH^2 + 0.031573 \times DBH^2 \times H \quad (6)$$

The volume function developed for birch trees by Braastad in 1967 (cited in Steinset T. A & Det Norske skogselskap 1999) was used for calculating the volume of all broadleaved tree species. The formula of Braastad was found to predict volume poorly for smaller broadleaved trees, and since there was no available volume function for small broadleaved trees, the volume-function for smaller pine trees was used instead. The volume function by Braastad was used for broadleaved trees with a *DBH* greater than or equal to 8 cm. Equation 7 is a formulation of Braastad's equation giving the output in dm^3.

Broadleaved trees with a *DBH* greater than or equal to 8 cm:

$$Volume = -1.86827 + 0.21461 \times DBH^2 + 0.01283 \times DBH^2 \times H \\ +0.0138 \times DBH \times H^2 - 0.06311 \times H^2 \quad (7)$$

DBH distributions

DBH distributions, later referred to as diameter distributions, were created with 5-cm *DBH* classes. A negative exponential function was fitted for each plot and year to ease the detection of deviations from an evenly falling diameter distribution.

This negative exponential function from Lundqvist et al. (2014) was fitted:

$$N_d = c_1 e^{-c_2 d} \quad (8)$$

Nd is the number of trees in *DBH* class *d*, while *c1* and *c2* are parameters to be estimated.

Ingrowth

Ingrowth in trees per ha and year, was calculated for each plot. When calculating the ingrowth per year, a period length of 10.5 years was used between 2004 and 2014, because the measurements were done at different times of the year setting the two measurements about 10.5 years apart. A period length of 6 years was used between 2014 and 2020. For the selection system plots, the period lengths that were used were the increment periods given in table 7. Ingrowth in the KONTUS sites had been registered in the field as all new trees above breast height, but the number of ingrowth trees presented in this thesis is new trees growing past a *DBH* of 2.5 cm. This was done in order to apply the same definition of ingrowth in the KONTUS and the selection system plots.

The planting instruction from Aulie (2013) and coordinates registered during that study were used to determine which of the ingrowth trees in sites 1-3 that were planted in 2004.

Mortality

Mortality in the KONTUS plots was calculated by summing up the number of trees which were registered as dead in 2014 and 2020.

In the selection system plots, it was not as easy to identify dead trees as the trees marked as dead could either be dead, felled, or missing. Felled trees had the code "6". Some trees were categorised as felled even though there had been no actual selective cutting. These were assumed to be single trees removed by people and thus were not included in the mortality calculations. Missing trees had a comment suggesting the tree was missing. All trees which were not felled or missing and within the category of dead trees were assumed to be dead.

The annual mortality was calculated in trees ha^{-1} $year^{-1}$, in %, and in m^3 ha^{-1} $year^{-1}$. When finding the mortality in trees ha^{-1} $year^{-1}$, period lengths of 10.5 years between 2004 and 2014 and 6 years between 2014 and 2020 were used for the KONTUS plots. In the selection system plots, the period lengths between registrations are given in table 7. Mortality in % was the number of dead trees in percent of the total number of trees in the plots. This was divided by

the period length since the last measurement, to estimate the percentage of trees that died per year between two measurements. The volume of dead trees per year (m^3 ha^{-1} $year^{-1}$) were also calculated by summing the volume ha^{-1} of all trees identified as dead and dividing by the period length since the last measurement.

Increment periods

Increment periods between measurements were calculated for each plot in order to calculate the annual increment between two measurements. Since trees grow during the growing season, these periods were estimated from the number of growing seasons between measurements.

For the KONTUS plots, there were six years between the measurements in 2014 and 2020. Since both registrations were in the summer during the growing season at about the same time, the increment period between these measurements was 6 years. The increment period between 2004 and 2014 was 10.5 years since the registration in 2004 was before the growing season.

For the selection system plots, the number of growing seasons between measurements were more difficult to estimate. Based on results from Mäkinen et al. (2008), which suggested that diameter increment for spruce begins in June and ends in the beginning of August, increment periods were estimated to the nearest 0.5 years (Table 7).

Table 7: Increment periods for the selection system plots.

Plot	Date of measurement	Increment period (years)
36	20.08.1977	
36	01.-02.08.1990	13
36	09.-11.06.2015	24
61	27.06.1990	
61	13.06.2001	11
61	04.09.2013	13
90	18.09.1990	
90	05.-13.09.2005	
90	04.-15.05.2020	14
145	23.-24.08.79	
145	04.-05.07.1990	10.5
145	12.-19.06.2015	25
178	13.08.1990	
178	06.-07.06.2001	10
329	09.1989	
329	20.-23.06.2000	10.5
329	09.-11.06.2009	9
453	13.06.1989	
453	26.-29.06.2000	11

Volume increment

Stand-level volume increment was calculated as *GVI* and NVI. Gross volume increment (*GVI*) is the periodical annual change in gross volume (standing, harvested, and dead trees) and net volume increment (NVI) is the periodical annual change in net volume (gross volume minus dead trees). In this study, *GVI* and *NVI* were calculated based on the status and volume increment of individual trees between two registrations.

GVI thus only included the increment of living trees (including ingrowth), whereas *NVI* corrected *GVI* for trees changing status from living to dead. The calculations of the *GVI* and *NVI* between two registrations (reg.) are shown below.

GVI was calculated as shown below:

$$GVI = \frac{\left(Volume\ living\ trees\ reg.2 - (Volume\ living\ trees\ reg.1 - volume\ harvested\ trees\ reg.2)\right)}{Increment\ period\ length} \quad (9)$$

The volume increment of the living trees between two registrations had to be corrected for the harvested trees. Even though trees had been registered as harvested in registration 2, they might have been harvested in any time between the two registrations. In this study, trees were assumed to have been harvested at the beginning of the increment period. The volume in registration 1 of the trees registered as harvested in registration 2 was therefore removed from the increment.

NVI was then calculated as shown below:

$$NVI = GVI - \frac{Volume\ of\ dead\ trees\ reg.2}{Increment\ period\ length} \quad (10)$$

Size-growth relationship

The size-growth relationship was plotted for each plot and year with relative cumulative tree volume on the x-axis and relative cumulative tree volume increment on the y-axis. Trees were sorted by volume, from lowest to highest. The cumulative volume for each tree was the sum of the volume of the tree itself and all trees with a lower volume than the tree in question. The cumulative volume of the last tree in the order was equal to the sum of the volume of the plot. The cumulative volume increment was found by summing in a similar way. Cumulative volume and cumulative volume increment were transformed from absolute to relative values by dividing by the plot totals. A 1:1-line was added to the plots, which indicates that all trees contribute to the volume increment proportional to their size.

From these size-growth plots, the Gini index was calculated, a single number describing how much the observed line differed from the 1:1-line (Bellù & Liberati, 2006). The Gini index was calculated as the area between the observed line and the 1:1-line, Area A, divided by the total area above the 1:1 line, Area A + Area B (Figure 4).

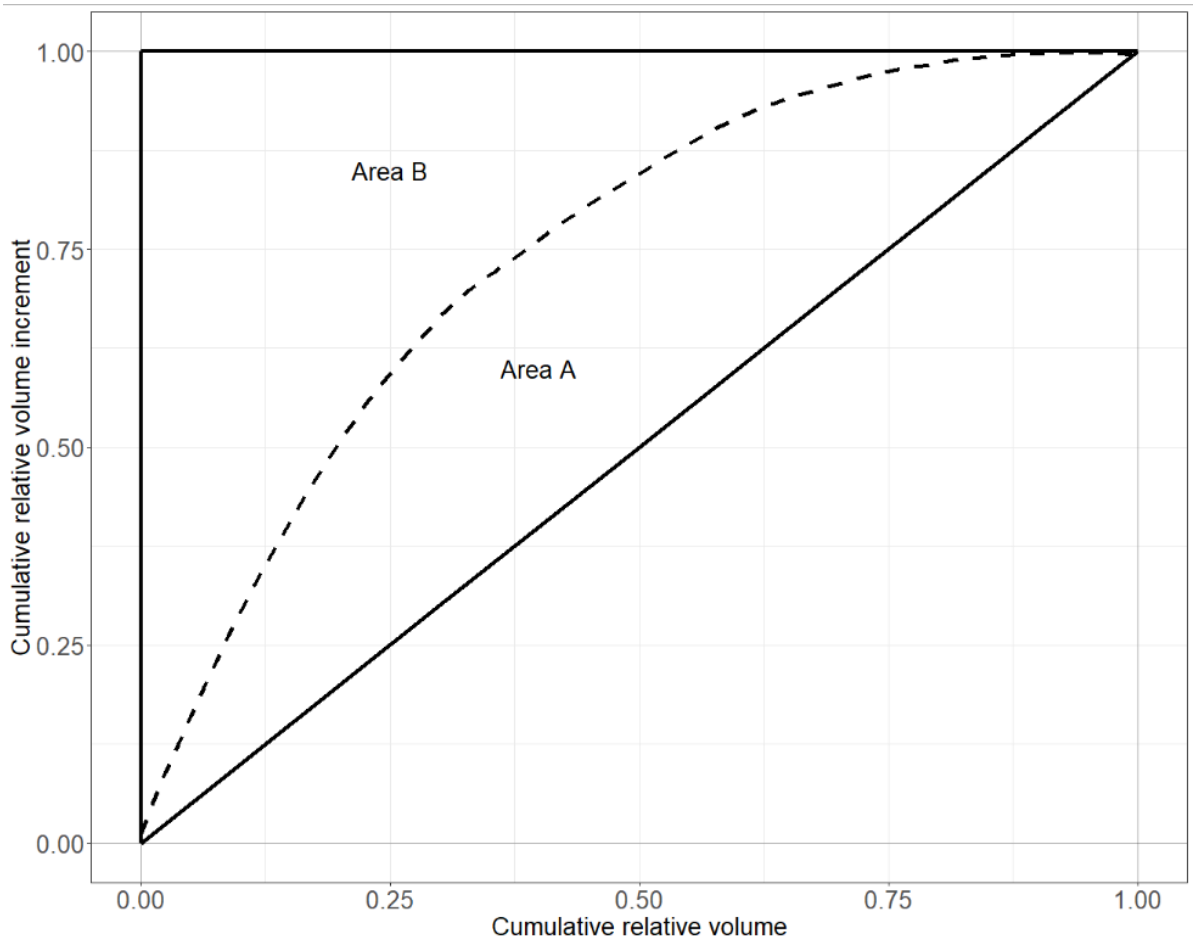

Figure 4: Concept for calculating the Gini index.

This Gini index is very similar to calculations of the dominance coefficient (Forrester, 2019; West, 2014), the difference being whether the values are positive or negative. In this study, there were only observed lines over the 1:1-line and Gini indices were therefore redefined to only take on positive values between 0 and 1. A higher value for the Gini index is an indication that the size-growth relationship is more concave.

Statistical analysis

Volume increment and stand density

Models were made to quantify the relationship between density (volume) and volume increment in terms of *GVI* and *NVI*. To test what shapes *GVI* and *NVI* would yield, and if these shapes were in line hypothesis 3, models were made with stand volume, site index and Gini index as possible independent variables. The stand volume, hereby called *volume* (m^3 ha^{-1}), was added to describe the effect of stand density in the model. *Site index* (m) was added because growth level varies with site index. The *Gini index* was added to the model to test whether a level of concavity of the size-growth relationship would affect volume increment.

One model was fitted with *GVI* (m^3 ha^{-1} $year^{-1}$) as the response variable and another with *NVI* (m^3 ha^{-1} $year^{-1}$) as the response variable.

Only spruce plots were used to fit the model, and the data from site 3 was therefore excluded. In the model for *NVI*, data from site 6 and plot 90 were excluded because in both cases there was exceptionally high mortality compared to what one would normally expect. In site 6, the death of one big tree explained almost all the mortality and contributed a large proportion of the total volume on this small plot. In plot 90 there had been large amounts of windfall in the northern part of the plot as a consequence of harvesting of the neighbouring stand.

The non-linear models were based on models by Allen et al. (2020), which have the flexibility to give shapes like increasing, optimum, or asymptotic. Allen et al. (2020) applied this model with basal area and site index as independent variables. In this analysis, volume was used instead of basal area and another parameter, *a02*, was added to include the effect of the Gini index.

The basic model with the only independent variable being density (expressed as *volume*):

$$NVI\ or\ GVI = a0 * Volume * \exp\left(-\frac{Volume}{a1}\right) \quad (11)$$

Site index and *Gini index* were added as independent variables in the following form:

$$NVI\ or\ GVI = (a0 + a01 * Site\ Index + a02 * Gini\ index) * Volume * \exp\left(-\frac{Volume}{a1}\right) \quad (13)$$

Mortality and stand density

A linear model was fitted to test whether *volume* (m^3 ha^{-1}) had a significant effect on *mortality* (m^3 ha^{-1} $year^{-1}$) (Equation 14). Similarly to the model for *NVI*, data from site 6 and plot 90 were excluded from the analysis because of the exceptionally high mortality.

$$Mortality = \beta_0 + \beta_1 \times Volume \quad (14)$$

Ingrowth and stand density

To test hypothesis 1, a linear model was fit to see whether density expressed as *volume* (m^3 ha^{-1}) had a significant effect on the number of ingrowth trees (*ingrowth*, trees ha^{-1} $year^{-1}$) (Equation 15). Only ingrowth trees that had been regenerated naturally, i.e. not planted, were included in the regression. Plots of *ingrowth* over *volume* suggested that the relationship was non-linear. Therefore, *ingrowth* was log-transformed using the natural logarithm. In plot 329, there were no ingrowth trees in the measurement of 2008. Since it is impossible to take the logarithm of 0, the number 1 was added to all observations before log-transformation (equation 15).

$$\ln(Ingrowth + 1) = \beta_0 + \beta_1 \times Volume \quad (15)$$

Results

In this section, the results relating to hypotheses 1, 2, and 3 are presented. First, results relating to hypothesis 1 will be presented, followed by the analysis of mortality. Then results related to hypothesis 2 will be presented and finally there will be a presentation of the results relating to hypothesis 3. Some of the tables and figures might not relate to the hypotheses directly but are helpful in interpreting the results.

Stand density

The number of trees, basal area, and volume for the KONTUS and the selection system plots are given in tables 8 and 9. These are different measures for the stand densities at the plots. The density expressed as basal area and volume increased over time for all plots, while the number of trees increased over time for most plots.

The volume (m^3 ha^{-1}) was the measure of density that was used in the analyses. In the analyses of density, the volume in the beginning of the measurement period was used. This means that only densities from year 2004 and 2014 for the KONTUS plots and from registration 1 and 2 in the KONTUS plots were used in the upcoming analyses. For these years, a majority of the plots had densities (volumes) between 100-200 m^3 ha^{-1}.

Table 8: Stand density as number of trees (ha^{-1}), basal area (m^2 ha^{-1}), and volume (m^3 ha^{-1}) for the KONTUS plots in all registration years. Numbers are calculated for living trees with a DBH greater than or equal to 2.5 cm.

Site	Plot	Number of trees (ha^{-1})			Basal area (m^2 ha^{-1})			Volume (m^3 ha^{-1})		
		2004	2014	2020	2004	2014	2020	2004	2014	2020
1	1	860	855	870	15.2	19.0	21.1	124	163	185
1	2	1265	1240	1200	20.6	26.0	28.5	164	224	255
2	1	825	1060	1100	19.5	24.2	26.8	143	180	203
2	2	1070	1440	1540	16.9	22.7	24.3	117	161	176
3	1	805	880	1265	12.7	17.9	20.7	98,7	145	169
3	2	865	1055	1205	10.3	14.6	16.6	68,6	101	116
4			820	910		17.9	20.3		156	179
5			1060	1070		19.4	21.8		158	182
6			1100	1130		28.3	30.0		282	306
7			1180	1320		14.7	17.1		108	131

Table 9: Stand densities as number of trees (ha^{-1}), basal area ($m^2\ ha^{-1}$), and volume ($m^3\ ha^{-1}$) for the selection system plots. For registration years for the given numbers, see table 4.

Plot	Number of trees (ha^{-1})			Basal area ($m^2\ ha^{-1}$)			Volume ($m^3\ ha^{-1}$)		
Registration	1.	2.	3.	1.	2.	3.	1.	2.	3.
36	443	1383	1593	14.7	23.4	35.4	120	197	339
61	994	1003	1213	18.4	23.4	27.7	151	205	258
90	1300	1262		22.3	30.5		224	319	
145	394	1053	1976	13.9	18.5	31.7	120	149	290
178	909	947		20.3	24.5		159	200	
329	1078	1277	1200	15.1	19.6	23.2	97.1	128	161
453	808	905		22.2	29.7		185	250	

Ingrowth

The ingrowth was analysed and related to the density (volume) in the plots to answer hypothesis 1.

The average ingrowth was 20.4 trees ha^{-1} $year^{-1}$, and the variation in the number of ingrowth trees was large, spanning from 0 to 72.9 trees ha^{-1} $year^{-1}$ (Table 10, Table 11). In most plots it was an adequate amount of ingrowth. About 75% of the observations of the ingrowth numbers in table 10 and table 11 were above 10 trees ha^{-1} $year^{-1}$.

For most plots, the number of ingrowth trees that were planted was low, but in site 3 plot 1 there were more planted trees than ingrowth trees which had not been planted. It was believed that these planted ingrowth trees did not take up so much space that they were preventing establishment of new natural regeneration, and also that they were so small that there was no competition for resources with naturally regenerated ingrowth. This meant that the planted ingrowth was probably not influencing the ingrowth caused by natural regeneration, and naturally regenerated ingrowth in these plots could be used in further analyses.

Two plots had especially high levels of ingrowth, plot 36 in 1990 and plot 145 in 1990. These plots had a variation in the spatial distribution of trees with gaps in the stand (Appendix 1) which might have made it easier for trees to grow past the *DBH* threshold.

Table 10: Ingrowth (trees ha^{-1} year^{-1}) in the KONTUS plots. The ingrowth in trees ha^{-1} year^{-1} is calculated separately for ingrowth that is planted, and ingrowth that is not planted. Years mark the beginning of the period.

KONTUS plots					
Stand	Plot	Ingrowth, not planted (trees ha^{-1} year^{-1})		Ingrowth, planted (trees ha^{-1} year^{-1})	
		2004	2014	2004	2014
1	1	10.95	5.83	0.476	2.50
1	2	15.24	4.17	2.38	0.833
2	1	24.8	8.33	2.86	1.67
2	2	44.3	21.7	2.38	9.17
3	1	17.6	19.0	1.43	33.3
3	2	21.4	13.8	0.952	7.50
4	4		16.7		
5	5		6.67		
6	6		20.0		
7	7		25.0		

Table 11: Amount of ingrowth (trees ha^{-1} year^{-1}) in the selection system plots. Registration is a representation of the measurement year which differed between the plots (see table 4). Registration numbers mark the beginning of the period.

Selection system plots		
Plot	Ingrowth (trees ha^{-1} year^{-1})	
Registration	1.	2.
36	72.9	15.5
61	2.40	22.9
90	19.6	
145	63.8	41.0
178	10.2	
329	19.0	0.00
453	9.18	

The regression analysis showed that stand density (*volume*) did not explain the variation in naturally regenerated ingrowth. The number of naturally regenerated ingrowth trees showed no pattern over stand density, although the plots with the most ingrowth were only found at lower stand densities (Figure 5). Below 150 m^3 ha^{-1}, ingrowth varied from 0 to 73 trees ha^{-1} $year^{-1}$ while the variation in ingrowth was lower at higher densities. Whether stand density limits the possibility of high recruitment at densities above 150 m^3 ha^{-1} cannot be analysed with the given data, because there are too few observations above this density to detect a limiting effect of density on ingrowth. Hypothesis 1 was not confirmed by these results.

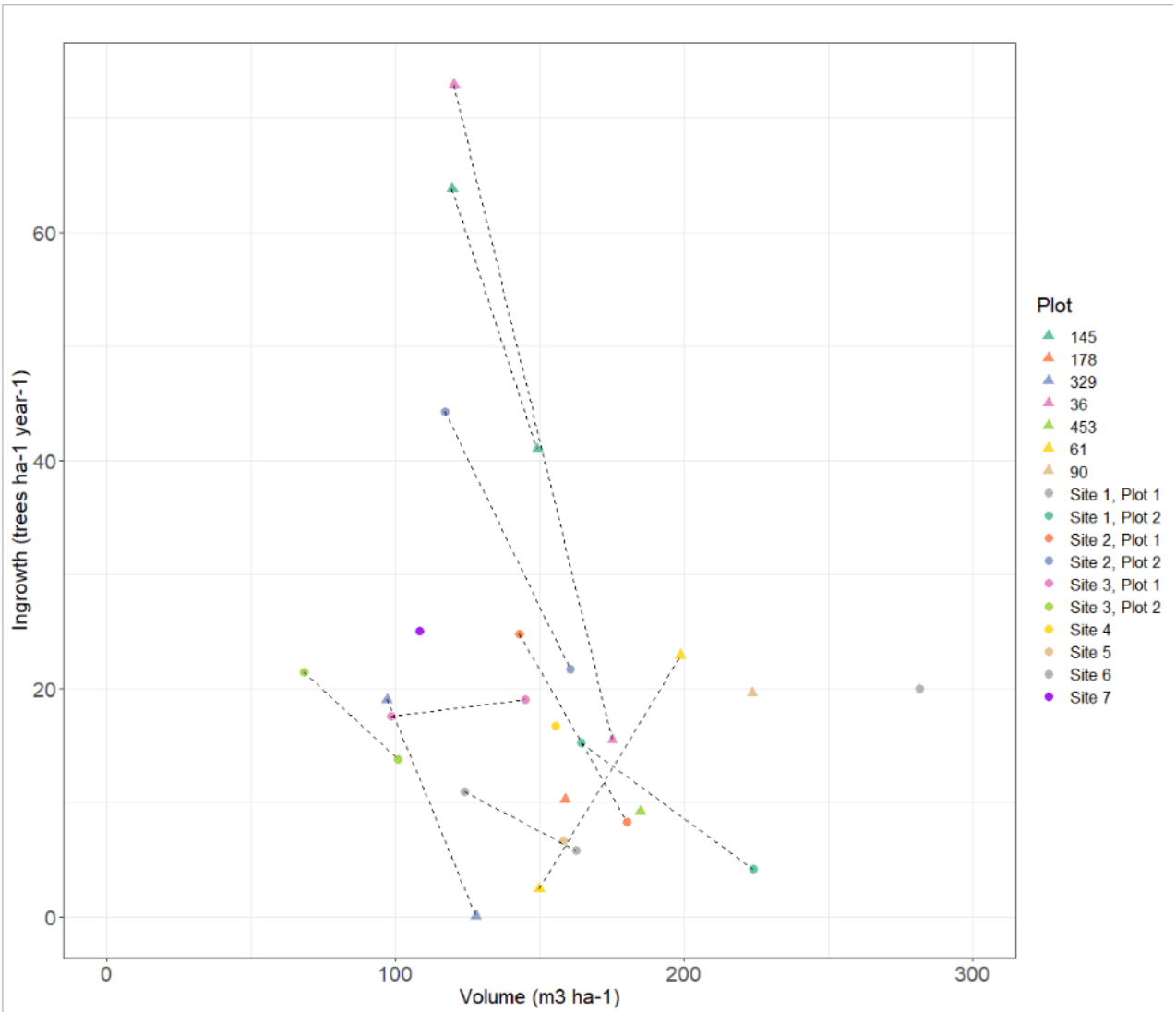

Figure 5: Ingrowth and stand density (volume). Dotted lines connect periods for the same plot. Only ingrowth trees regenerated with natural regeneration are included.

Mortality

The mortality of the plots and results from the regression of mortality and volume are presented below.

The mortality in the KONTUS and the selection system plots was generally low (Figure 6, Table 12, Table 13). The average mortality was 4.89 trees ha^{-1} $year^{-1}$ or 0.29% (Table 12, Table 13). Although the mortality ranged from 0 to 24.5 trees ha^{-1} $year^{-1}$ and between 0-1.23%, most observations were far below the extremes. Around ¾ of the observations of mortality were lower than 6.46 trees ha^{-1} $year^{-1}$ and 4 %.

Even though the mortality generally was low, some plots had distinctly higher mortality than most other plots. Plot 90 had an especially high mortality compared to the other plots, while site 6 had the highest relative mortality of 1.23 %. This can also be seen in Figure 6 where the mortality in volume is displayed. In plot 90, the mortality was caused by frequent windfall as a consequence of clear-cutting the neighbouring stand. On site 6, one large tree had died and since the area of the plot was small, the death of this tree caused mortality. The mortality of these two plots were seen as the most extreme in the data. The mortality was on average 3.70 trees ha^{-1} $year^{-1}$ when excluding these two plots from the calculation.

Plot 178, plot 61 and site 2 plot 2 also had high mortality in terms of the volume in some years (Figure 6). In plot 178, a large proportion of the volume of dead trees was attributed to steam breakage, while in plot 61 most of the mortality was attributed to trees that had been uprooted. These are both results of wind or snow damage. In site 2 plot 2, the mortality was much higher in 2020 than in 2014. Mortality was also almost exclusively limited to one half of the plot, and there were comments of some uprooted trees and stem breakage on living trees. This might suggest that wind has played a role in the mortality of this plot.

Table 12: Mortality for the KONTUS plots. Years mark the beginning of the period.

KONTUS plots					
Stand	Plot	Mortality (trees ha^{-1} $year^{-1}$)		Mortality per year (%)	
		2004	2014	2004	2014
1	1	6.19	4.17	0.673	0.466
1	2	6.19	10.8	0.474	0.856
2	1	0.476	2.5	0.0447	0.224
2	2	0.952	11.7	0.0657	0.725
3	1	0.00	0.833	0	0.0656
3	2	1.43	3.33	0.134	0.272
4			1.67		0.181
5			5.00		0.455
6			15.0		1.23
7			1.67		0.125

Table 13: Mortality for the selection system plots. Registration is a representation of the measurement year which differed between the plots (see table 4). Registration numbers mark the beginning of the period.

Selection system plots				
Plot	Mortality (trees ha^{-1} $year^{-1}$)		Mortality per year (%)	
Registration	1.	2.	1.	2.
36	0.385	3.75	0.0107	0.104
61	1.54	5.44	0.0459	0.163
90	24.5		0.739	
145	1.11	8.12	0.0305	0.222
178	6.46		0.322	
329	0.0771	8.45	0.00208	0.228
453	0.353		0.0192	

The regression analysis revealed no significant effect of stand density (*volume*) on mortality. Plot 90 and Site 6 were not included in the regression analysis because their mortality was much higher than the other plots. Plot 178, plot 61 and site 2 plot 2 were kept in the model even though their mortality was relatively high.

The mortality in terms of volume was low. When not including the five plots with signs of wind and snow damage marked with text in Figure 6, the mortality only ranged between 0 and 0.6 m^3 ha^{-1} $year^{-1}$, and there seemed to be no increase in mortality with increasing density. The average mortality in the plots was 0.32 m^3 ha^{-1} $year^{-1}$ if plot 90 and site 6 were excluded from the calculation.

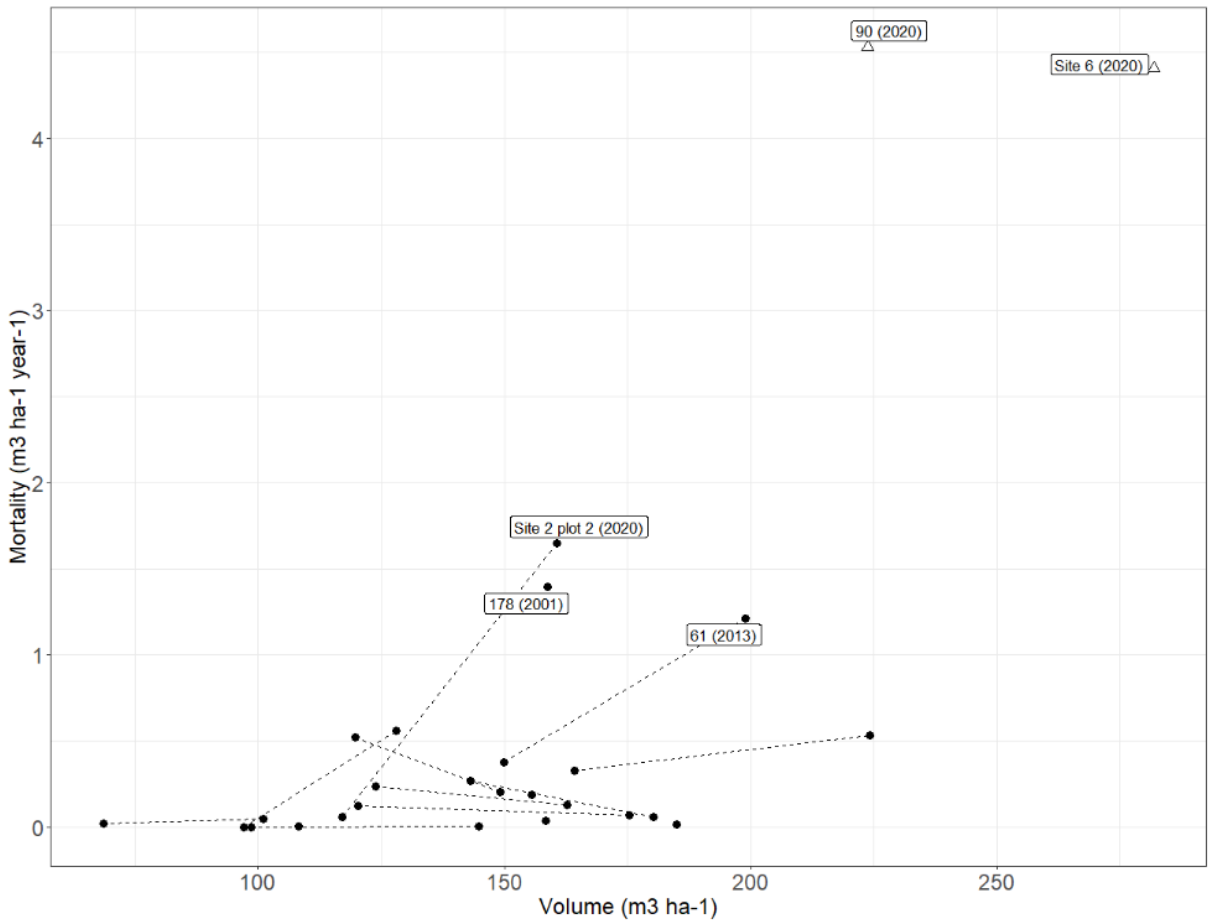

Figure 6: Mortality (m^3 ha^{-1} $year^{-1}$) over volume (m^3 ha^{-1}) for each plot. Three plots had high mortality, but were still included in the regression model, and their plot names are given in the figure. Empty triangles are data from site 6 and plot 90 which were not included in the regression model.

Stand structure

In the following section, results relating to hypothesis 2 are presented. The spatial distribution of trees and diameter distributions are presented and discussed since this information is helpful for understanding the size-growth relationships. At the end of the section, the size-growth relationships and Gini indices will be presented, directly relating to hypothesis 2.

Spatial distribution of trees

The spatial distributions of trees might help explain differences in volume increment, because they show whether individual trees have space to grow and if they are in competition with other trees.

Appendix 1 contains maps of the spatial distribution of trees at the last registration for all plots. At the KONTUS and selection system plots, the spatial distribution was heterogeneous with some aggregation of trees. Ingrowth was found most often in gaps but were also growing under larger trees. In the KONTUS plots, the non-ingrowth trees were sparsely distributed with some larger parts of the stands having very few non-ingrowth trees. In the selection system plots, there were seemed to be larger differences between plots concerning the distribution of non-ingrowth trees. Some plots like plot 61 and plot 178 seemed to have many non-ingrowth trees leaving less room for ingrowth. In plot 178 these non-ingrowth trees had quite similar sizes, making the plot more homogeneous. Plot 36 and 145 differed from the other selection system plots, by having much fewer non-ingrowth trees. The reason why only non-ingrowth trees are discussed here, is that these trees have the most potential to affect growth by competing with other trees for resources.

Diameter distributions

Diameter distributions are a way of displaying the stand structure or size-distribution in a stand. The size-distribution might affect the size-growth relationship, as seen in Figure 1. Diameter distributions are not the same as the size-distributions in Figure 1 and will not affect the size-growth relationship in the same way, but they are also a way of displaying which sizes of trees that are the most numerous.

The KONTUS plots had falling diameter distributions, although there were some deviations from the negative exponential function (Figure 7). Especially site 1 plot 1, site 1 plot 2 and site 4 had more trees in the mid-range of the diameter distributions than the negative exponential function implied. The variation in the diameter distributions was small between registrations, indicating that the structure of the stands remained stable. The most pronounced difference between registrations was more ingrowth in 2020 for site 1 plot 1, site 3 plot 1, site 4, and site 6. In general, the number of trees was often lower in the first diameter class compared to the second diameter class, because the width of this diameter class was only 2.5 cm while the other diameter classes had widths of 5 cm.

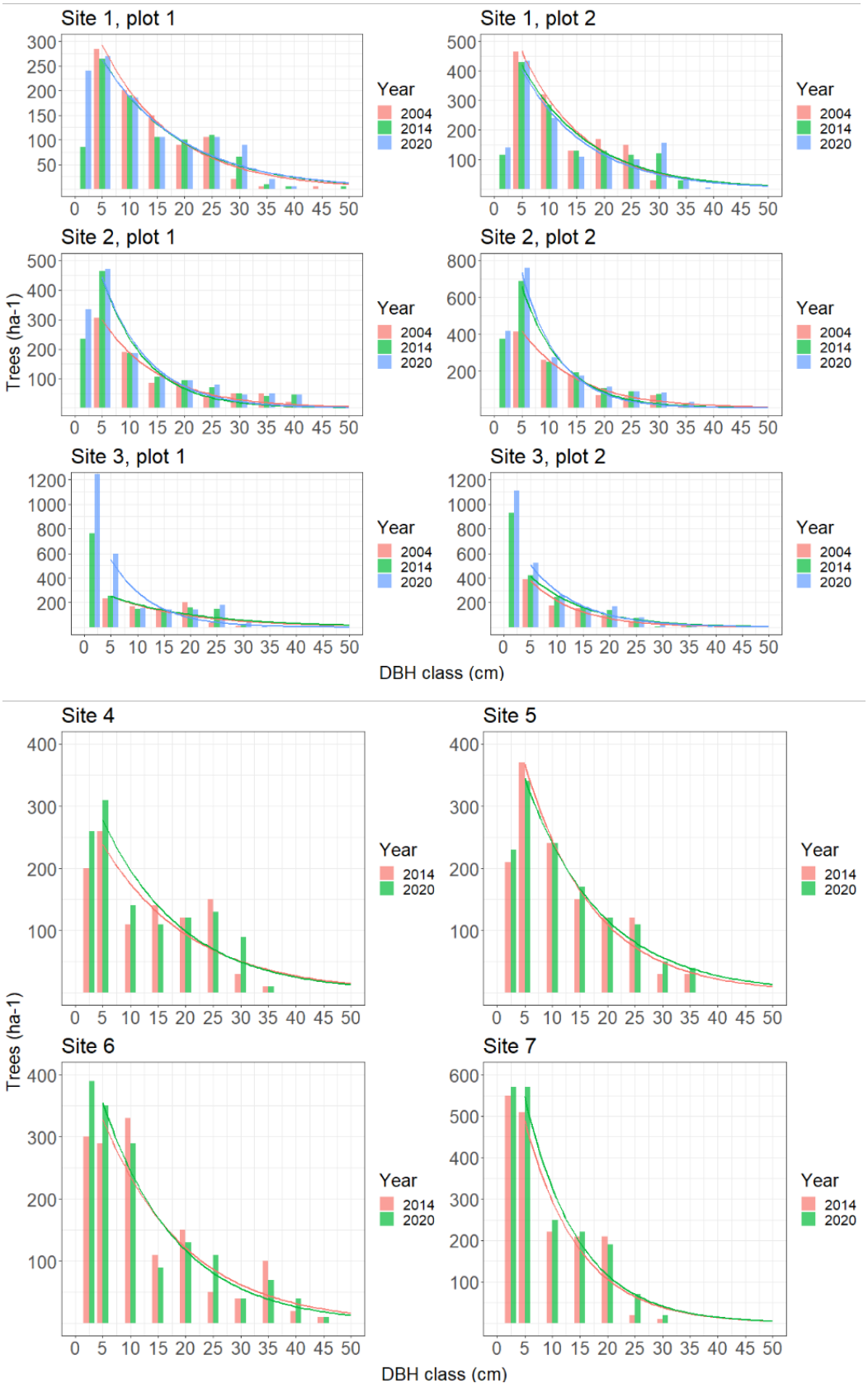

Figure 7: Diameter distributions in the KONTUS plots on sites 1-7 for all registration years. DBH class 5 spans from 2.5-7.5 cm, DBH class 10 spans from 7.5-12.5 etc. Trees in the first column between DBH 0 and 5 were trees with a DBH below the 2.5-cm threshold. Negative exponential functions were fitted for the DBH distributions of each registration year for trees with DBH > 2.5 cm.

The selection system plots also had mostly falling diameter distributions (Figure 8, Figure 9), and the distribution of some plots like 145 and 90 resembled an inversed J-shape. Plot 178 was the only plot that had a bell-shaped diameter distribution (Figure 9), which set this diameter distribution apart from all other diameter distributions in this study. The map of plot 178 (Appendix 1) also shows that many of the trees had similar sizes and that there was little room for new ingrowth trees to emerge. Plots 61 and 453 had diameter distributions which were closer to a linear decrease than an exponential decrease. Most plots that changed their diameter distribution between measurements, changed in the direction of more ingrowth trees and a more distinct falling diameter distribution. These changes were perhaps the largest for plot 36 and 145 where the maps (Appendix 1) show that the non-ingrowth trees were sparsely distributed leaving more room for new ingrowth trees.

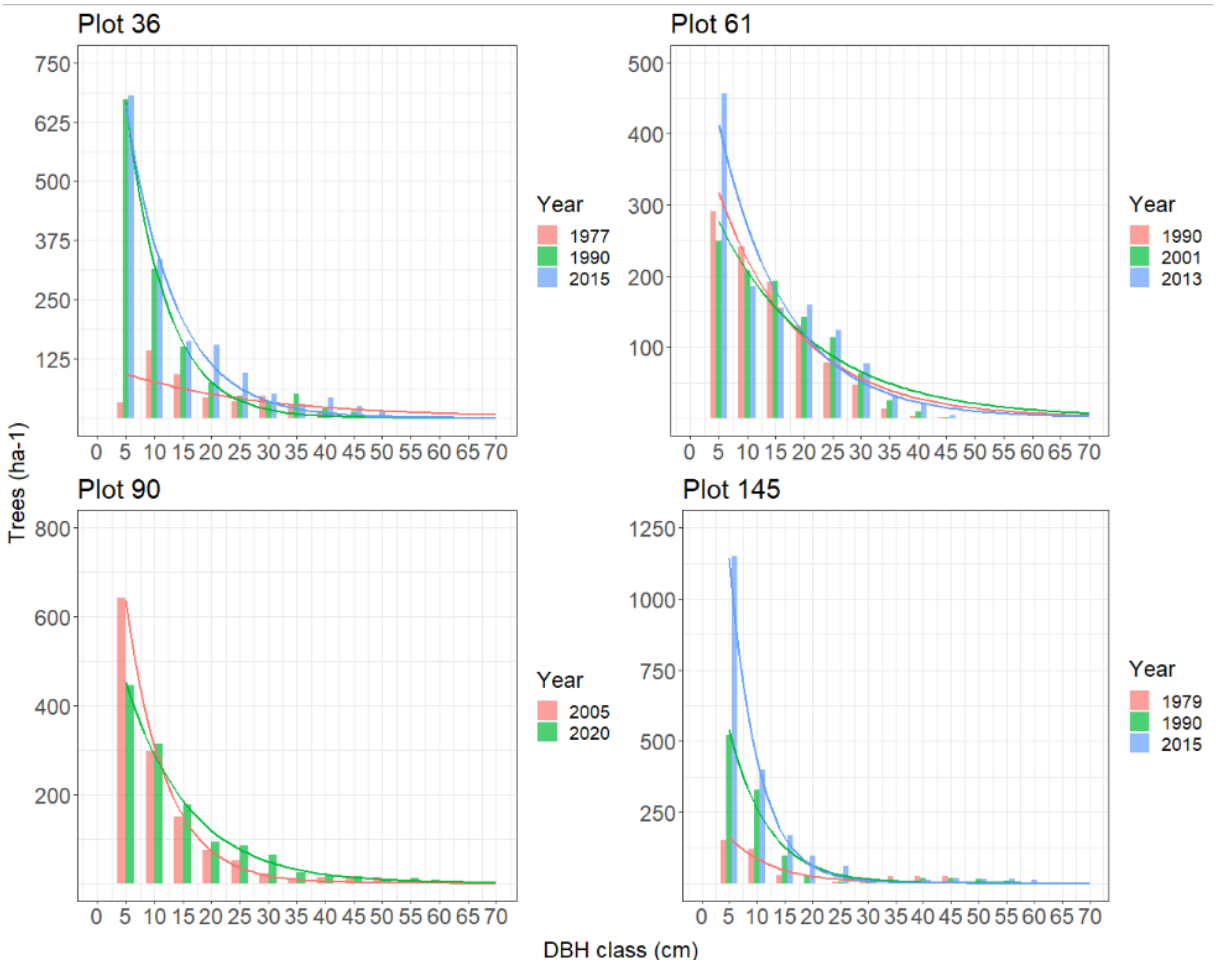

Figure 8: Diameter distributions in the selection system plots on plot 36, 61, 90 and 145 for all registration years. DBH class 5 spans from 2.5-7.5 cm, DBH class 10 spans from 7.5-12.5 etc. Negative exponential functions were fitted for the DBH distributions of each year for trees with DBH > 2.5 cm.

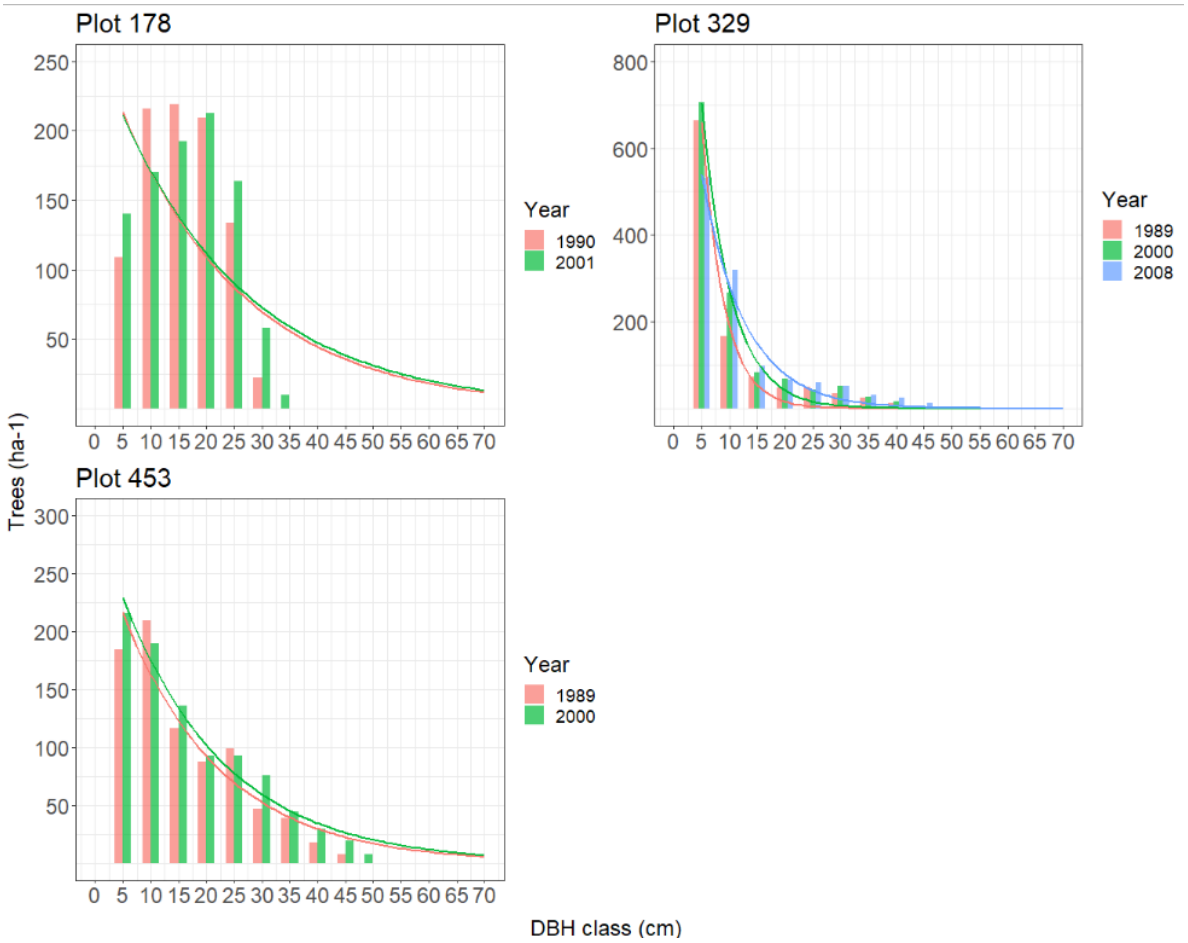

Figure 9: Diameter distributions in the selection system plots on plot 178, 329 and 453 for all registration years. DBH class 5 spans from 2.5-7.5 cm, DBH class 10 spans from 7.5-12.5 etc. Negative exponential functions were fitted for the DBH distributions of each year for trees with DBH > 2.5 cm.

Size-growth relationship

The size-growth relationships and Gini indices for the plots are presented in Figures 10-14. Most plots had a concave size-growth relationship, and the average Gini index was 0.252. There were only 4 observations of Gini indices bellow 0.1 and most plots had a Gini index above 0.2.

The plot with the highest Gini index was plot 90 (Figure 14). In this plot, around 65% of the cumulative volume increment was reached at a cumulative volume of 25%. This means that ¼ of the proportion of the stand volume which belonged to the trees with the lowest volumes, produced about 65% of the volume increment in the plot. It is possible that the unusually high Gini index in this plot was influenced by the harvest in 2005 where 111 m^3 ha^{-1} was removed (Table 3). Site 2 plot 2, plot 36, plot 145, and plot 329 had the highest Gini indices if omitting plot 90. These plots also had falling diameter distributions that coincided well with the negative exponential functions (Figure 7, Figure 8, Figure 9).

A few plots, Site 1 plot 2, Site 4, and Site 7 had size-growth relationships, which were close to the 1:1-line. The Gini indices for these plots were also quite low, being 0.0473 to 0.0527,

0.0886 and 0.0725 for Site 1 plot 2, Site 4, and Site 7, respectively. One can hardly say that there was a concave size-growth relationship in these plots.

The size-growth relationships also varied between periods for the same plot. In Site 1 plot 1, site 2 plot 2, and plot 329, the size-growth relationships moved closer to the 1:1-line (Figure 10, Figure 11, Figure 14) while in plot 36, there was an opposite trend, and the curve was further away from the 1:1-line in 1990 than in 1977 (Figure 13). However, these variations were not substantial enough to change the shape of the size-growth relationships.

Most of the KONTUS and the selection system plots had concave size-growth relationships. Some plots did not have a concave size-growth relationship and while there is no reason to doubt the validity of the results from these plots, this only occurred in 3 of in total 17 plots. Most of the data was in support of hypothesis 2 and indicated that the proportion of the volume belonging to the smallest trees have a higher relative volume increment than the proportion of the volume belonging to larger trees. Hypothesis 2 was supported by these results.

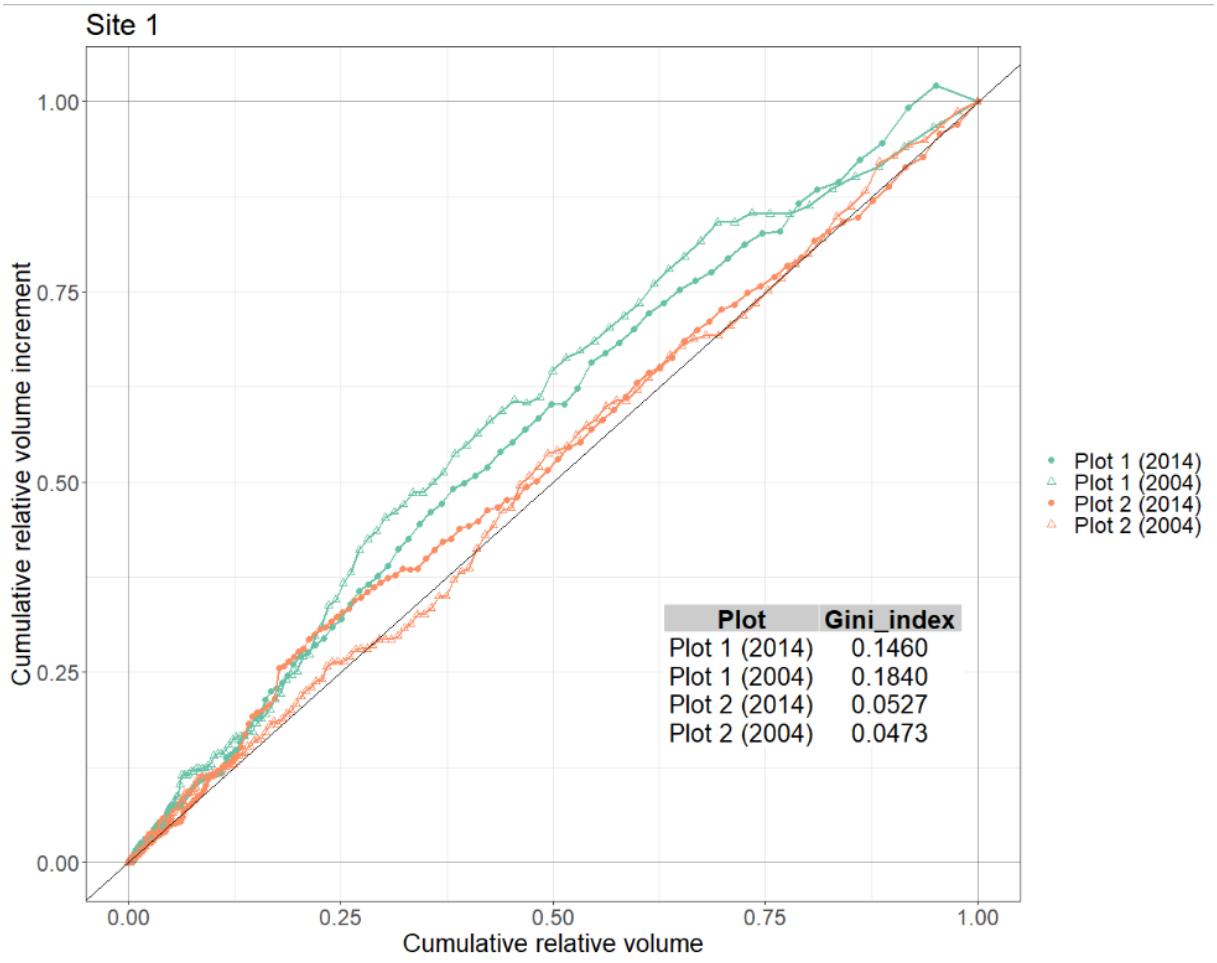

Figure 10: The size-growth relationships, which is the relationships between the cumulative relative volume and the cumulative relative volume increment, and the Gini indices in the KONTUS sites, Site 1.

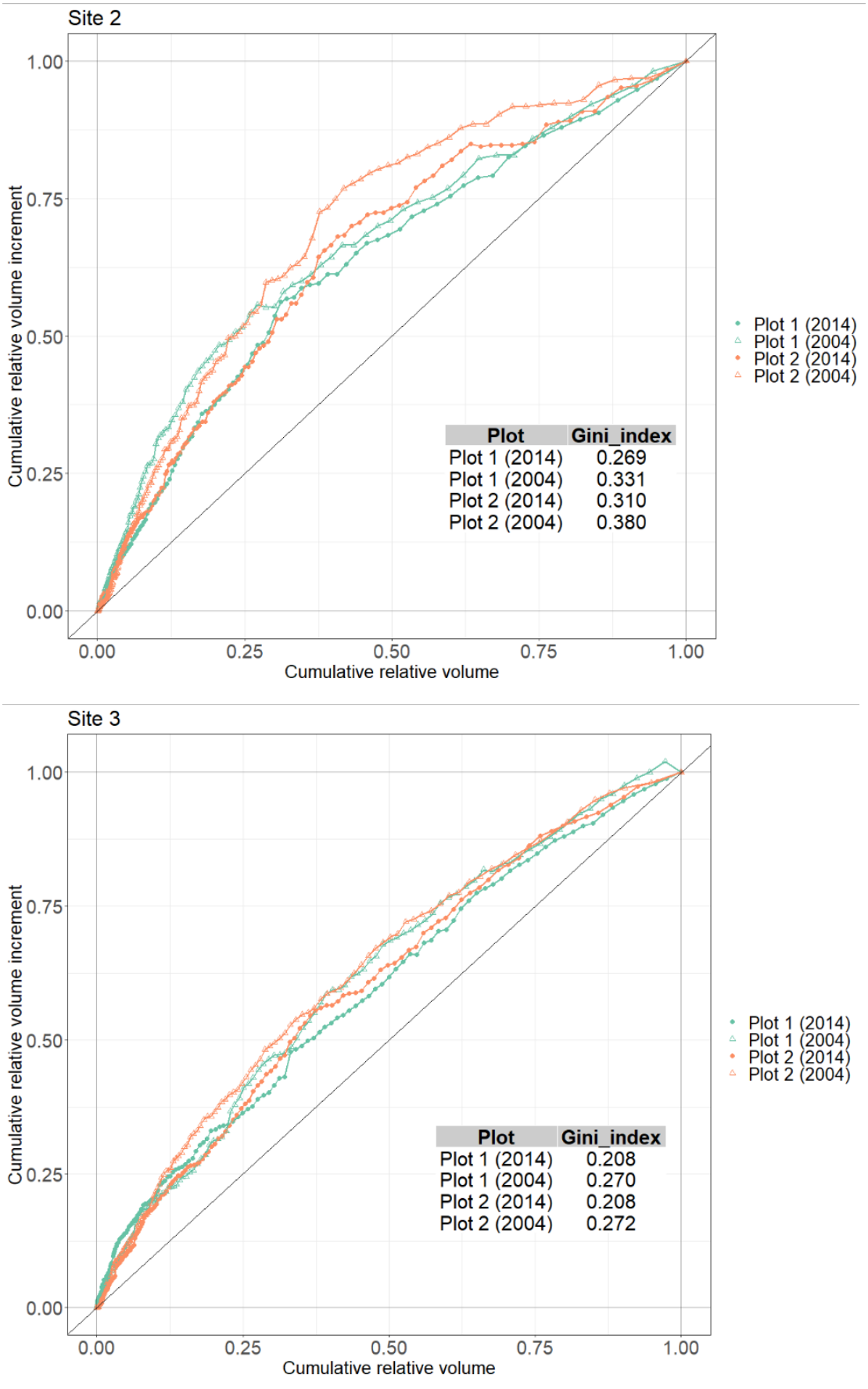

Figure 11: The size-growth relationships, which is the relationships between the cumulative relative volume and the cumulative relative volume increment, and the Gini indices, in the KONTUS sites, Site 2 and Site 3.

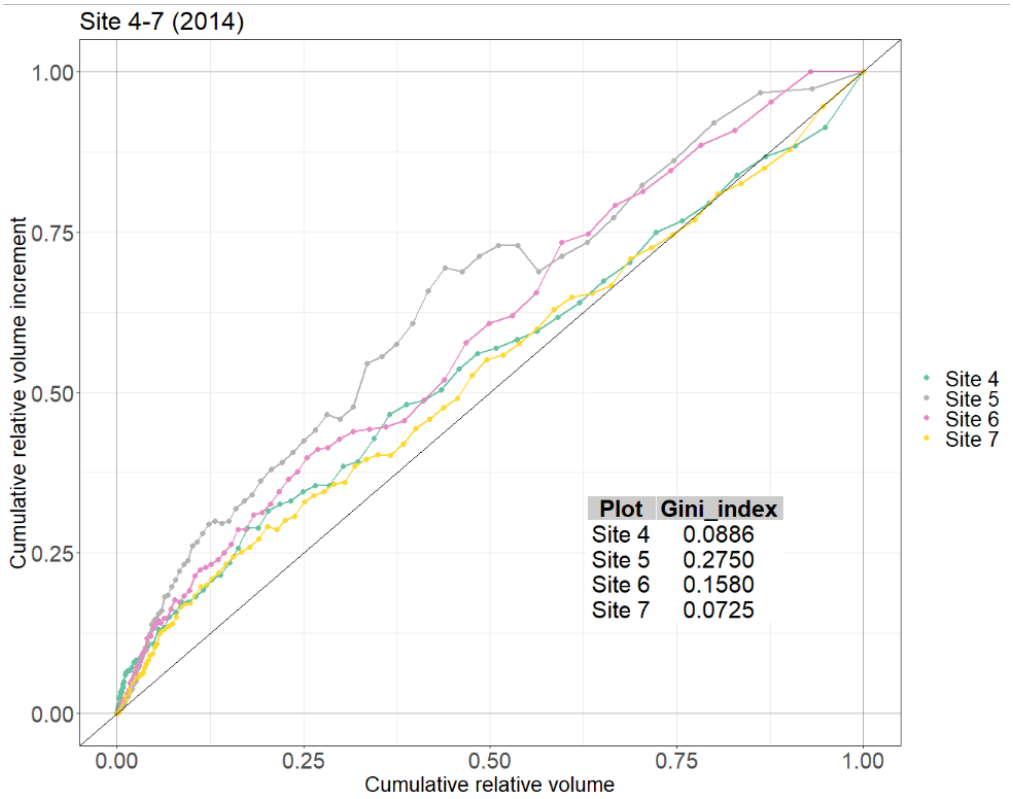

Figure 12: The size-growth relationships, which is the relationships between the cumulative relative volume and the cumulative relative volume increment, and the Gini indices, in the KONTUS Sites 4-7.

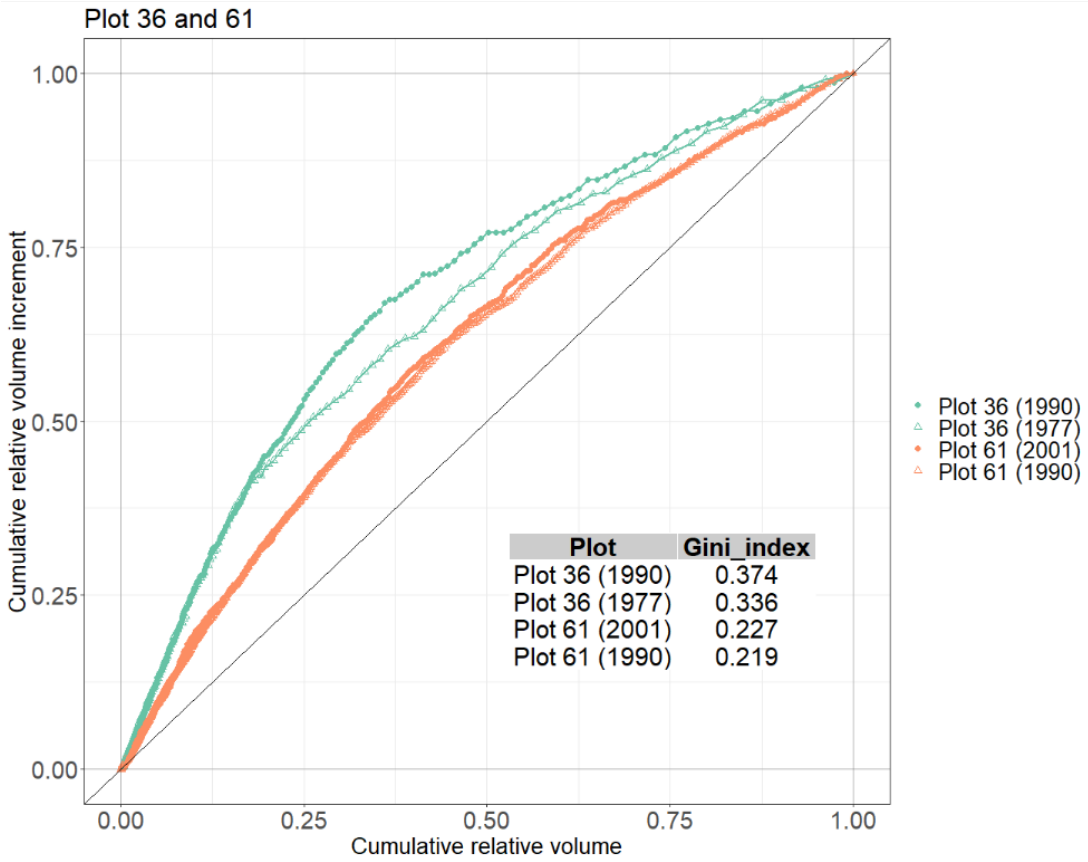

Figure 13: The size-growth relationships, which is the relationships between the cumulative relative volume and the cumulative relative volume increment, and the Gini indices, in the selection system plots 36 and 61.

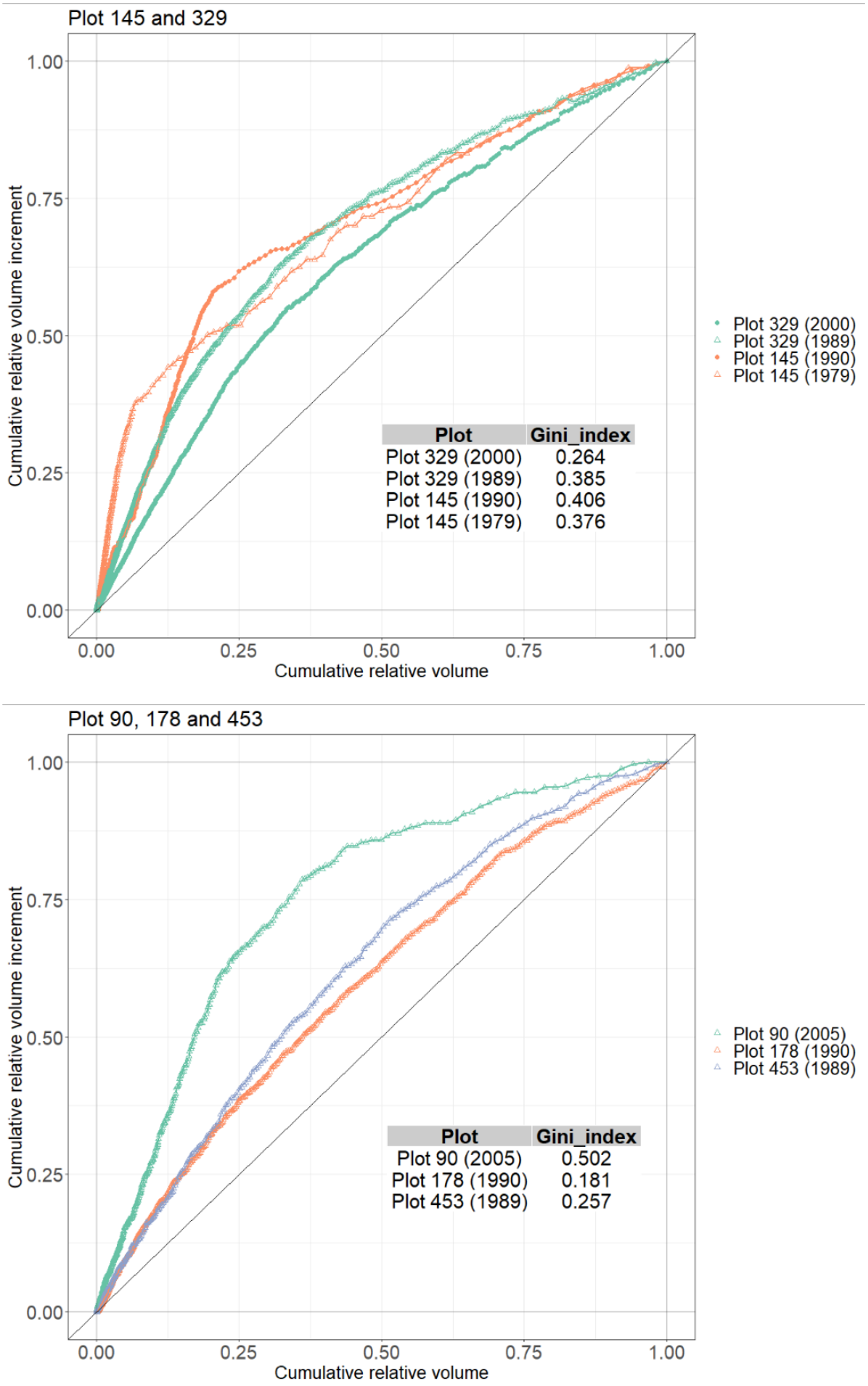

Figure 14: The size-growth relationships, which is the relationships between the cumulative relative volume and the cumulative relative volume increment, and the Gini indices, in the selection system plots 145 and 329, and the selection system plots 90, 178, and 453.

Volume increment and stand density

Tables 14 and 15 contain the values for *GVI* and *NVI* which were the response variables in the models describing how density affected volume increment. *GVI* varied greatly, and the plots with the highest *GVI* had values of around 6 m^3 ha^{-1} $year^{-1}$. *NVI* was slightly lower than *GVI* for most plots since most plots had low mortality (Figure 6). Still there were some plots where the differences between *GVI* and *NVI* were substantial. In site 6, the *NVI* was negative since the mortality in 2020 was higher than the ingrowth and volume increment between 2014 and 2020.

Table 14: Gross volume increment (m^3 ha^{-1} $year^{-1}$) and Net volume increment (m^3 ha^{-1} $year^{-1}$) for the KONTUS plots. Years indicate measurement periods. 2004 is the period between 2004 and 2014. 2014 is the period between 2014 and 2020.

Site	Plot	Gross volume increment (m^3 ha^{-1} $year^{-1}$)		Net volume increment (m^3 ha^{-1} $year^{-1}$)	
		2004	2014	2004	2014
1	1	3.69	3.74	3.46	3.61
1	2	5.70	5.16	5.37	4.63
2	1	3.53	3.75	3.26	3.70
2	2	4.16	2.57	4.10	0.92
3	1	4.40	4.00	4.40	4.00
3	2	3.10	2.56	3.07	2.51
4			3.88		3.69
5			3.94		3.90
6			3.95		-0.45
7			3.77		3.77

Table 15: Gross volume increment (m^3 ha^{-1} $year^{-1}$) and Net volume increment (m^3 ha^{-1} $year^{-1}$) calculated for the selection system plots. Periods 1 and 2 indicate measurement periods. 1 is the period between registration 1 and 2. 2 is the period between registration 2 and 3, see table 4 and table 7.

Plot	Gross volume increment (m^3 ha^{-1} $year^{-1}$)		Net volume increment (m^3 ha^{-1} $year^{-1}$)	
Period	1	2	1	2
36	5.91	6.83	5.79	6.76
61	4.96	4.58	4.59	3.37
90	6.77		2.24	
145	2.82	5.64	1.45	5.43
178	4.16		2.77	
329	2.95	3.72	2.94	3.15
453	5.87		5.86	

The final models which were chosen for the effect of density and site index on *GVI* and *NVI* are presented in Table 16 and Figures 15-17. The mathematical expressions of the final models for *GVI* and *NVI* were the same as Equation 13 but without the *a02* parameter since this parameter associated with the *Gini index* was not significant for *GVI* or *NVI*.

The *a01* parameter was significant in the *GVI* and the *NVI* model (Table 16). This parameter was associated with the *site index* indicating that this was an important variable in both models.

In the *NVI* model, the *a1* parameter was not significant. This was a sign that no optimum shape occurred (Allen et al., 2020). The *NVI* model still predicted an optimum shape, but the predicted optimum was outside the range of the data (Figure 16).

*Table 16: Parameter estimates and fit statistics for the models of GVI and NVI, equation 13. Only significant variables with parameter estimates. *= p-value < 0.05, ** = p-value < 0.01, *** = p-value < 0.001.*

	Parameter	Estimate	SE	*RMSE* (m^3 ha^{-1} $year^{-1}$)
GVI	*a01*	0.004577***	0.0007834	0.8956
	a1	209.0***	43.08	
NVI	*a01*	0.003878*	0.001433	1.265
	a1	229.6	121.4	

There were no trends in the residuals of the variables *volume* and *site index* which were included in the models (Figure 18, Figure 19). There were also no trends in the residuals for the *Gini index* which was not included in the model. Residual plots for the *Gini index* were still made to look for patterns that might suggest that this variable should be included in the model.

Figure 15 and Figure 16 show the data and model predictions of *GVI* and *NVI*.

Predictions were made for three site indices; 11.5, 13.5 and 15.5 that represented the low, medium, and high site indices in the data. Except for plot 90 which had a site index of 18, site indices in the KONTUS and the selection system plots ranged from 11-15.1 (Table 1, Table 2), and 11.5, 13.5 and 15.5 were chosen as site indices in the lowest, mid-range and highest range of the site indices in the data.

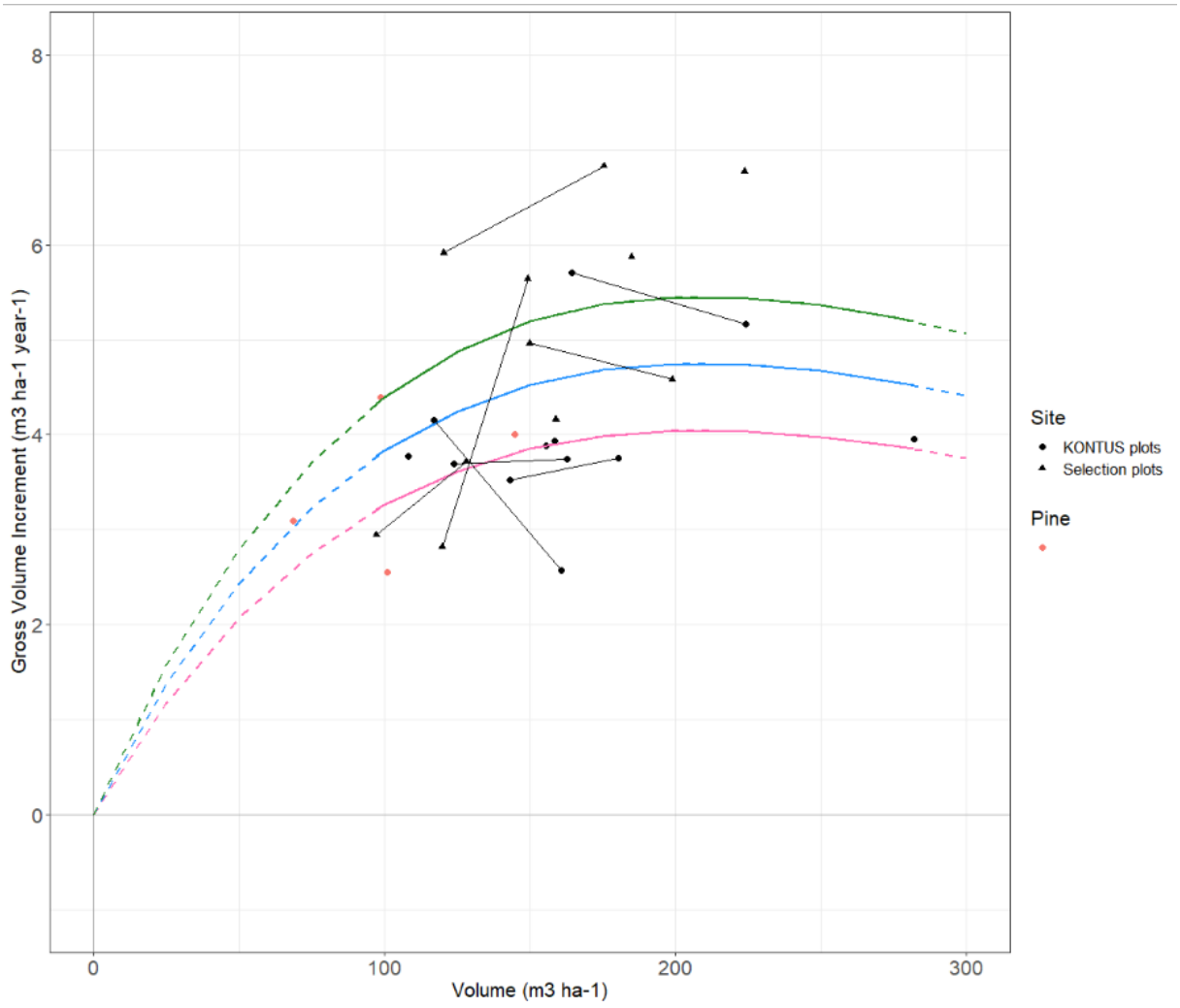

Figure 15: Model predictions for the GVI model for site indices 11.5 (pink), 13.5 (blue) and 15.5 (green). The dashed lines imply at which densities model predictions are outside the range of the data. Black dots and triangles are data from spruce-dominated plots used to fit the model. Red dots are from pine-dominated plots. Observations connected with lines are from different growth periods on the same plot.

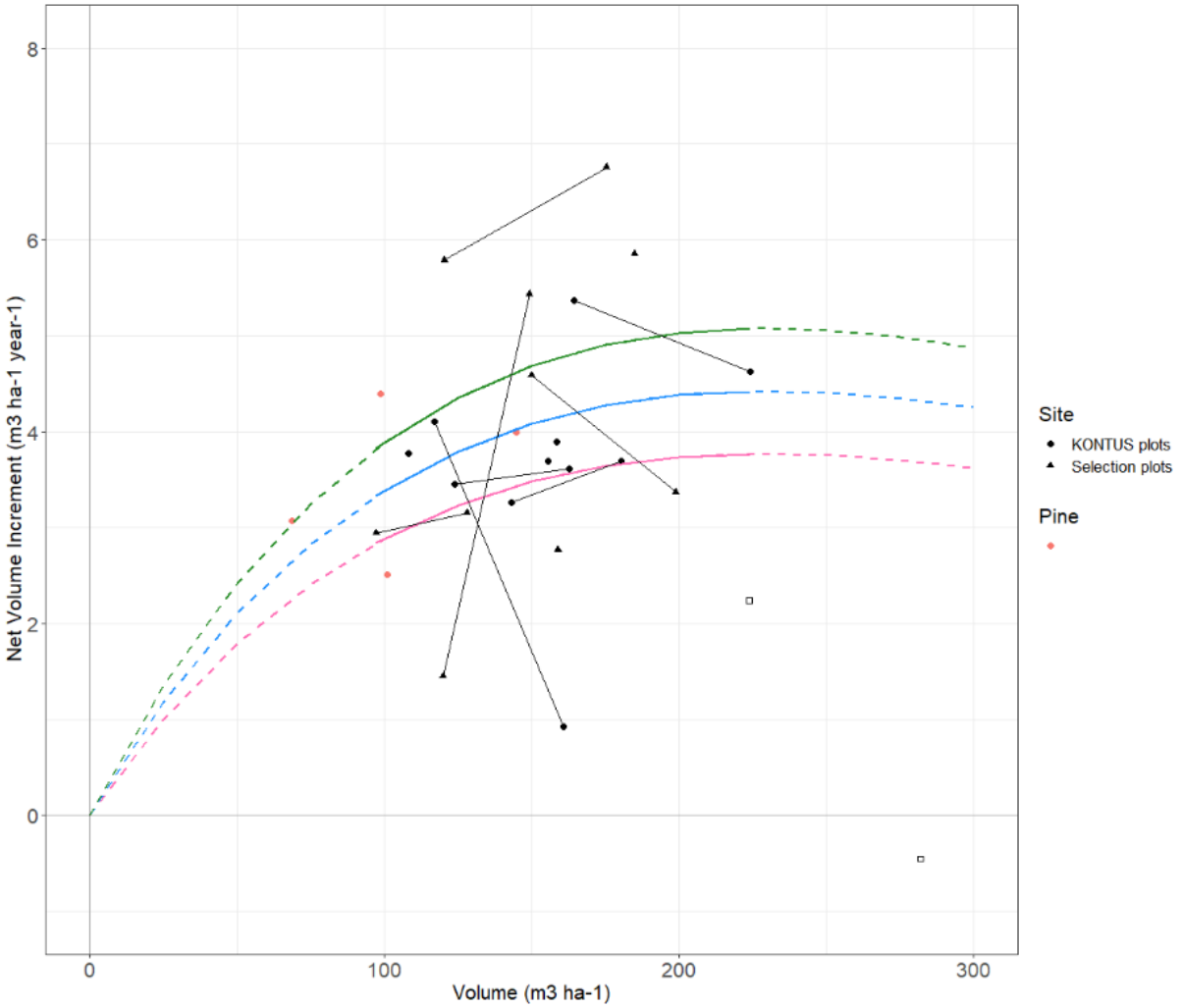

Figure 16: Model predictions for the NVI model with site indices 11.5 (pink), 13.5 (blue) and 15.5 (green). The dashed lines imply at which densities the model is outside the range of the data. Black dots and triangles are data from spruce-dominated plots used to fit the model. Red dots are pine data. Observations connected with lines are from different growth periods on the same plot. Empty squares are data from site 6 and plot 90 which were not included in the modelling data.

Predictions of *GVI* and *NVI* are compared with each other in Figure 17. The model predicted a *NVI* which was slightly lower than the *GVI*. The differences between predictions of *GVI* and *NVI* were caused by the mortality, and since the mortality was low for most plots (Figure 6), the predicted *NVI* was very close to the predicted *GVI* with the same *site index*.

The model for *GVI* predicted an optimum at 209 m^3 ha^{-1} (Figure 15), while the model for *NVI* predicted an optimum just outside the range of the data (Figure 16). There was not a lot of data to support the optimum predicted by the *GVI* model, since there were only three plots with a density of more than 200 m^3 ha^{-1}.

Hypothesis 3 stated that the relationship between *GVI* and density would be degressive. There was an optimum predicted by the *GVI* model, but this was uncertain, and the shape of the prediction curves were more resembling an asymptote than being degressive. Hypotheses 3 was not supported by the models describing the effect of stand density on *GVI* and *NVI*.

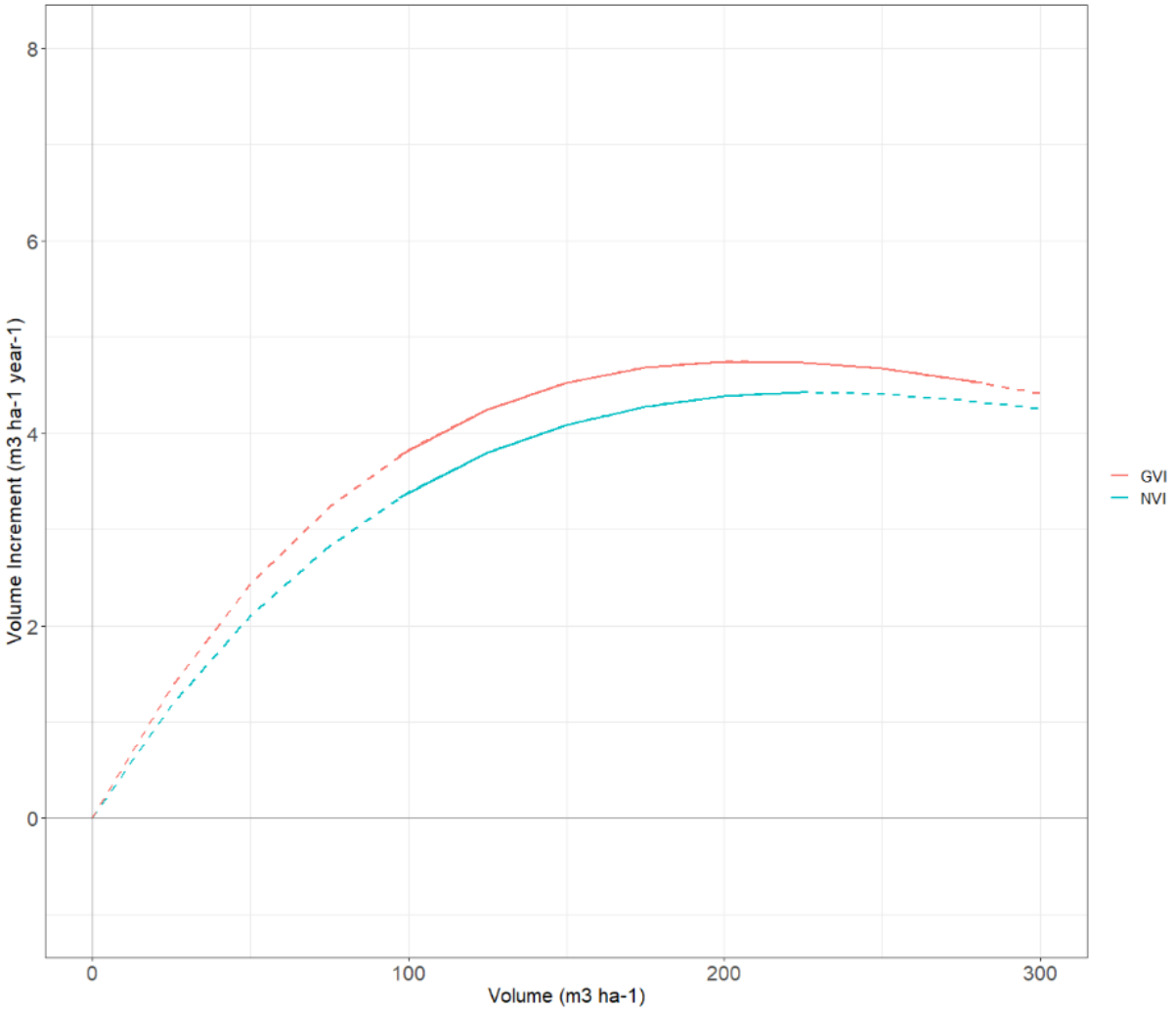

Figure 17: Model predictions of GVI and NVI with mean value for site index (13.5). The dashed lines imply at which volumes the predictions are outside the range of the data.

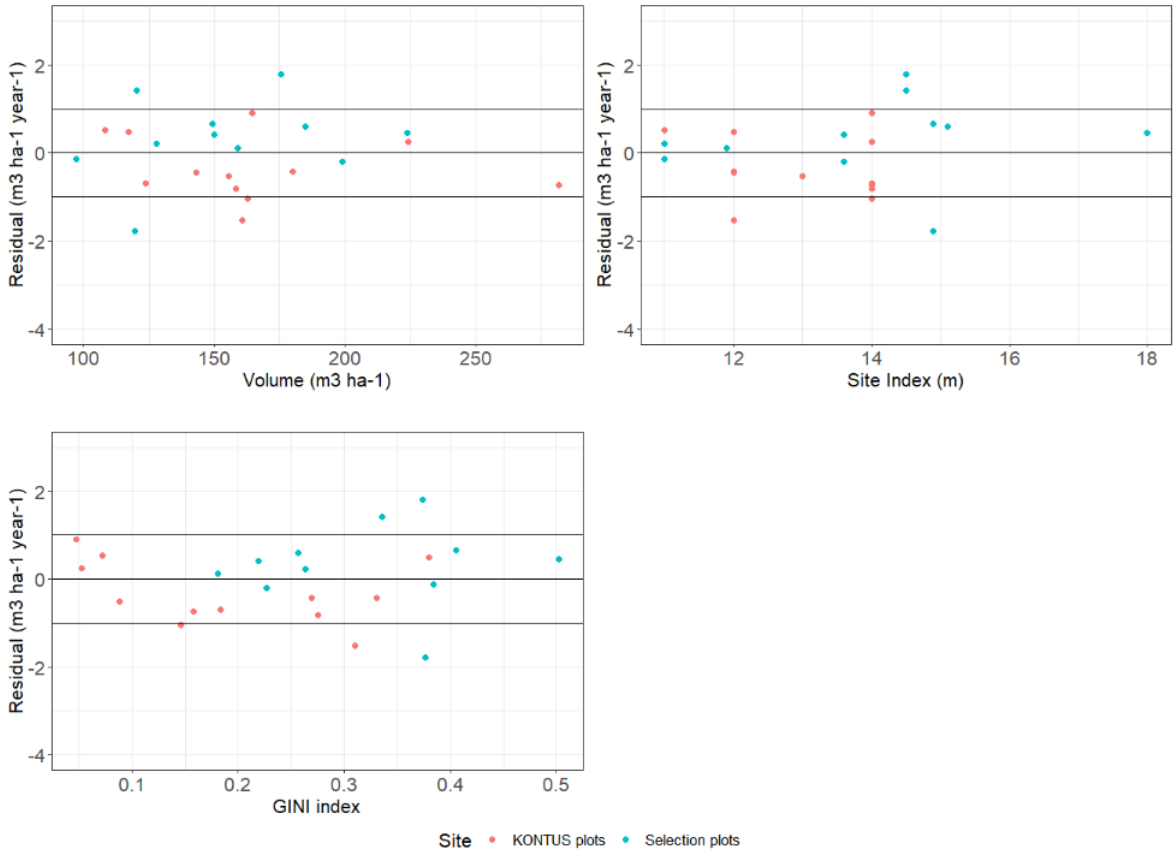

Figure 18: Residuals of the GVI model (Table 16).

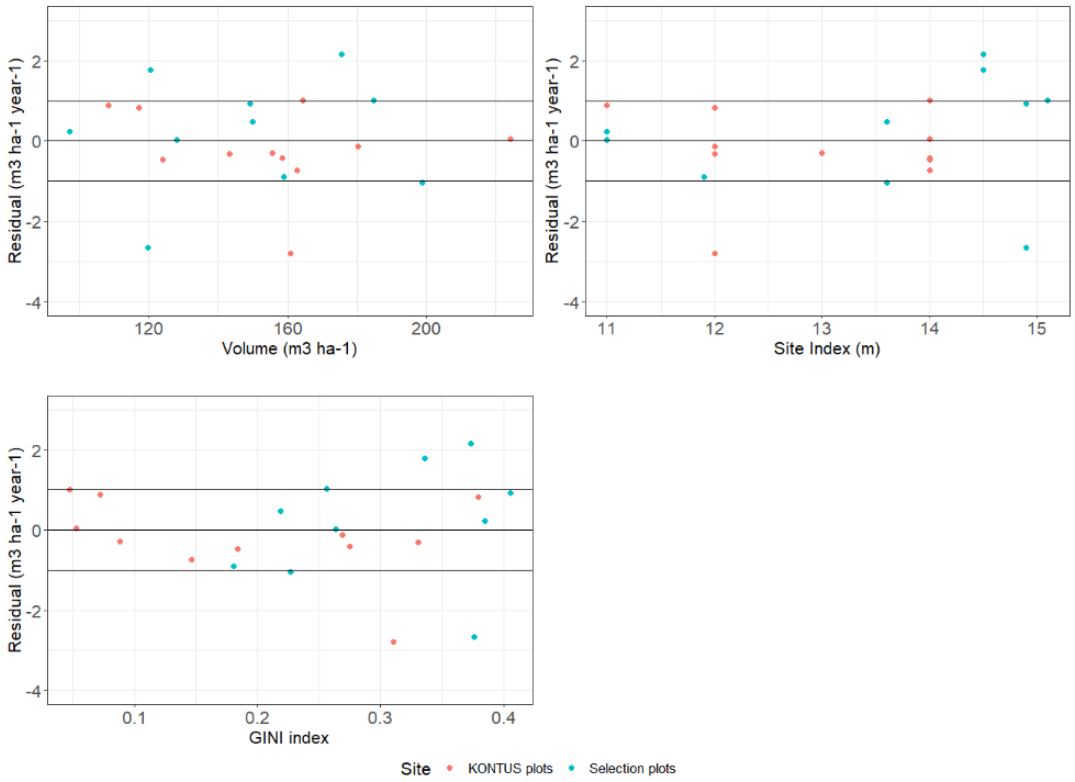

Figure 19: Residuals of the NVI model (Table 16).

Discussion

Volume growth in selectively cut and even-aged stands

The volume increment (Table 14, Table 15) is within the same range as earlier results from stands that have been selectively cut. Lähde et al. (2002) studied selectively cut stands and found a current annual increment (*CAI*) of on average 5.4 m^3 ha^{-1}. The plots in that study were spread across Finland, and *CAI* varied greatly from 3.05 to 9.24 m^3 ha^{-1}. In Lundqvist et al. (2007), the increment varied between 0.5 and 6.8 m^3 ha^{-1} $year^{-1}$ in Central and Northern Sweden. This also seems to be consistent with the results from the KONTUS and the selection system plots. However, even though the volume increment seems to be consistent with earlier studies, comparing the values of *GVI* and *NVI* with values of *CAI* in studies from other Nordic countries is difficult. This is because it is often not mentioned how the *CAI* is calculated. Site indices might also vary greatly between studies and there might also be different methods for quantifying the site index.

Lundqvist (2017) argues that *CAI* should, in theory, not change in forests managed by the selection system if the stand structure remains the same. Because of this, the mean annual increment (*MAI*) should equal *CAI* in selectively cut stands (Lundqvist, 2017). In this study, *CAI* was calculated for *GVI* and *NVI*, and *CAI* can be compared to the *MAI* of even-aged stands. A comparison between the growth in uneven-aged stands and even-aged stands can be done either by measuring the growth in these management systems side by side over a full rotation period, or by comparing uneven-aged stands with the *MAI* estimated by yield models for even-aged stands (Lundqvist, 2017).

The *MAI* for even-aged Norway spruce in Norway has been compiled by Tveite and Braastad (1981). They calculated the mean *MAI* for a variety of different simulated thinning programmes for a given site index. The site indices in the KONTUS and the selection system plots ranged between 11-18, and within this interval Tveite and Braastad (1981) calculated the mean *MAI* of site indices 11, 14, and 17.

The mean *MAI* of even-aged Norway spruce that was calculated by Tveite and Braastad (1981) was 3.5 m^3 ha^{-1} $year^{-1}$ for site index 11 while the *GVI* model predicted 3.9 m^3 ha^{-1} $year^{-1}$ for this site index at the optimal density (*volume*). With a site index of 14, the mean *MAI* was 5.5 m^3 ha^{-1} $year^{-1}$ while the *GVI* model predicted 4.9 m^3 ha^{-1} $year^{-1}$ at the optimal density. For site index 17, the mean *MAI* was 7.5 m^3 ha^{-1} $year^{-1}$ while the *GVI* model predicted 6.0 m^3 ha^{-1} $year^{-1}$ at the optimal density. The *RMSE* (m^3 ha^{-1} $year^{-1}$) in the *GVI* model was 0.8956, meaning that the average deviation between the prediction and the data was about 0.9 m^3 ha^{-1} $year^{-1}$. The *RMSE* is calculated in the same way as the standard deviation, but with a different meaning since it is an estimate for the error around a prediction and not the estimate for the error around a mean. For site indices 11 and 14 the difference between the *GVI* and the mean *MAI* was -0.4 m^3 ha^{-1} $year^{-1}$ and 0.6 m^3 ha^{-1} $year^{-1}$, respectively. These differences were lower than the *RMSE*, the average prediction error. For site indices 11 and 14, the difference between the predicted *GVI* and the mean *MAI* was very likely not statistically significant.

For site index 17, the difference between the mean *MAI* and the *GVI* was 1.5 m^3 ha^{-1} $year^{-1}$. In this case, it might be necessary to also consider uncertainty in Tveite and Braastad (1981). In Tveite and Braastad (1981) there was variation around the mean MAI, which was due to the different thinning programmes that were simulated. Although no numbers for the variation were given, the observations around the mean were plotted and the total range of these observations seemed to be slightly more than 1 m^3 ha^{-1} $year^{-1}$ for site index 17. If we return to the uncertainty associated with the *GVI*, it might be assumed that the residuals are normally distributed around the predicted value, although it should be noted that this assumption might not be true. If we consider that the *RMSE* is calculated in the same way as the standard deviation, then 68% of the observations should be within one standard deviation from the predicted value on either side and 95% of the observations should be within two standard deviations from the predicted value. Two standard deviations away from the predicted value is 1.8 m^3 ha^{-1} $year^{-1}$. Given the mentioned assumptions, 95% of the observations of the *GVI* should be within an interval of 1.8 m^3 ha^{-1} $year^{-1}$ on either side of the *GVI* that was predicted, which was 6.0. The difference between the mean *MAI* and the *GVI* for site index 17, which was 1.5 m^3 ha^{-1} $year^{-1}$, was within this range. Further, there is also uncertainty associated with the mean *MAI*.

The difference between *GVI* and the mean *MAI* for site index 17 was considerable. However, with available information about the uncertainty it cannot be concluded that the difference was statistically certain.

Andreassen (1994) also compared the growth in the selection system plots to the mean *MAI* in Tveite and Braastad (1981). Thus, some of the same plots were compared to the same value for the mean *MAI* in Andreassen (1994) and in the comparison above. However, the conclusions were very different. Andreassen (1994) concluded that the selection system plots on average produced 15-20% less than the mean *MAI*. A difference between the comparisons in this study and the one by Andreassen (1994) was that in Andreassen (1994) the densities in the selection system plots were used directly. It was not taken into consideration that these densities were probably not optimal. In this study of the KONTUS and the selection system plots, the optimal density predicted by the *GVI* model was used and the differences were not that big between *GVI* and mean *MAI* values for the same site index, perhaps with the exception of site index 17.

Stand density and ingrowth

The average ingrowth in this study was 20.4 trees ha^{-1} $year^{-1}$. Lundqvist et al. (2007) found an average ingrowth past the 5 cm *DBH* threshold of 21 spruce trees ha^{-1} $year^{-1}$ in central Sweden and 14 spruce trees ha^{-1} $year^{-1}$ in northern Sweden. Ahlström and Lundqvist (2015) found a mean ingrowth of 13.3 trees ha^{-1} $year^{-1}$ past 5 cm in *DBH* in the north of Sweden. Figures in Lundqvist et al. (2007) displaying the ingrowth (trees ha^{-1} $year^{-1}$) over volume (m^3 ha^{-1}) revealed that the variation in the number of ingrowth trees was large. Also, in Ahlström and Lundqvist (2015) there was a large variation in mean values of ingrowth for plots included in the study ranging from 8.1-21.7 stems ha^{-1} $year^{-1}$. Both Ahlström and Lundqvist (2015) and Lundqvist et al. (2007) point to earlier harvests as one reason for some of the

variation in ingrowth. This was probably not a relevant cause in the KONTUS and the selection system plots, since harvesting only occurred for a few plots (Table 6). In Lundqvist et al. (2007) there were some thinning treatments where a considerable amount of the volume was removed making it more difficult to compare to the KONTUS and the selection system plots.

Ingrowth did not decrease significantly with increasing volume which meant that hypothesis 1 was not confirmed by the results. This is in line with Lundqvist (2004), Ahlström and Lundqvist (2015) and Lundqvist et al. (2007), which did not find a significant relationship between standing volume and ingrowth in northern Sweden. It is not in line with the result from the plot in central Sweden in Lundqvist et al. (2007) where there was a significant negative effect of stand density. Ahlström and Lundqvist (2015) and Lundqvist et al. (2007) pointed to harvesting as a factor that seemed to affect the ingrowth rates in those studies, and that this factor sometimes correlated with the volume. Harvesting was not an issue in this study of the KONTUS and the selection system plots, except for in a few plots.

Stand structure and volume increment

There was a concave size-growth relationship for most of the plots, in line with hypothesis 2. This pattern has also been found in one of the plots in Castagneri et al. (2012) where the plot in question was a selectively cut spruce stand. Castagneri et al. (2012) mentioned less competition as a factor which might lead to a concave size-growth relationship. Some of the data in this study of the KONTUS and the selection system plots also seemed to be in support of this. Site 1 plot 2 had a particularly high density in terms of volume, a sign of more competition. The size-growth relationship was also close to the 1:1-line which might indicate that the stand was too dense for smaller trees to grow well.

Forrester (2019) discussed that both the stand density and stand structure might both be influencing the size-growth relationship. In the selection system plots, except from plot 90, the three plots with the highest Gini indices also had the lowest densities, but the differences between densities in the plots were generally small. A more prevalent pattern was that the plots with the highest Gini indices had falling diameter distributions that coincided well with the negative exponential functions. The spatial distribution might also have had an influence. Plots 36 and 145 had high Gini indices and the maps showed that there seemed to be sufficient room for growth of the smaller trees in the stand (Appendix 1).

The data from the KONTUS and the selection system plots indicated that density and structure influenced the size-growth relationships, but this is uncertain given that this was only interpretations from some observations in the data.

The size-growth relationship expressed as the *Gini index* did not explain any variation in volume increment, although the variation in *Gini indices* was large between plots. The residual plots (Figure 18, Figure 19) showed that there was no pattern when plotting the

residuals over *Gini index*. This indicated that there was no effect of the *Gini index* on *GVI* or *NVI*.

Stand density and volume increment

In other studies, it is rarely mentioned whether the increment that is studied is *GVI* or *NVI*. Because of this, and because the models of *GVI* and *NVI* had similar predictions (Figure 17), the *GVI* and *NVI* models will be discussed together in this section.

The models gave an optimum pattern for *GVI*, and the optimum was reached at 209 m^3 ha^{-1}. Still, the optimum shape predicted for *GVI* was only supported by three plots with a density above 200 m^3 ha^{-1}. Within the range of the data, the shape of the curve only increased slightly. This was not in line with hypothesis 3 which claimed that the relationship between stand density and *GVI* would be degressive.

Chrimes (2004) found an optimum curve when modelling selectively cut Norway spruce stands in Sweden. The model in that study used other variables, among them competition variables, but the optimum in that study was reached at around the same density (volume) of 197 m^3 ha^{-1}. The harvesting method applied was diameter limit-cutting which was the most comparable harvesting method compared to the harvesting in this study. Chrimes (2004) also reported of almost no data above 200 m^3 ha^{-1} where the optimum was reached and suggested that the formation of competition variables and the lack of data for higher densities was the reason for the decline after the optimum. The optimum pattern in Chrimes (2004) was uncertain as well, like in this study of the KONTUS and selection system plots.

Mortality

There was no significant effect of stand density (volume) on mortality in the regression model. This was also found by Valkonen et al. (2020) that studied the mortality in selectively cut stands in Southern Finland. In the KONTUS and selection system plots, larger mortality was on some plots caused by wind and snow damages. Still those damages only hit some plots, or parts of plots at random and had no apparent connection to the management system or the stand density. In Valkonen et al. (2020) wind and snow were also the two most important causes of death at the tree level, being the cause of death for 11% and 16% of the number of trees, respectively, while the reasons for death could not be identified in 55% of cases. Wind was the most important cause of death on the volume level.

In this study of the KONTUS and the selection system plots, the average mortality was 0.32 m^3 ha^{-1} $year^{-1}$ when plot 90 and site 6 which had exceptionally high mortality were excluded from the calculation. Valkonen et al. (2020) also reported of two incidents with exceptionally high mortality, and when the observation periods containing these events were removed from the calculation, they found an average mortality of 0.21 m^3 ha^{-1} $year^{-1}$. Valkonen et al. (2020)

had two observations with an annual mortality between 1-2 m^3 ha^{-1} $year^{-1}$ while in this study of the KONTUS and the selection system plots, there were three observations of mortality in this range (Figure 6). Valkonen et al. (2020) did, however, have many more observations in the low range, which might imply that the observations of high mortality had more of an impact on the average in this study of the KONTUS and the selection system plots because of sample size and not necessarily because of differences at the sites.

Conclusion

This study addressed how growth, ingrowth, and mortality in selectively cut stands might be affected by stand density and stand structure in selectively cut stands. The results showed no significant effect of stand density (volume) on ingrowth or mortality.

The plots that were studied often had a concave size-growth relationship. Stand density, stand structure, and harvesting might have affected this shape although harvesting was only a factor in two of the plots. The size-growth relationship expressed as the Gini index did not explain variation in stand volume growth.

Although there was a weak optimum shape in the *GVI* model, the shapes of the *GVI* and *NVI* models were closer to being asymptotic. These results were contrary to most other studies that have assessed the relationship between volume increment and density in selectively cut stands. Volume increments at optimal density were similar to the mean *MAI* from growth models for even-aged stands.

References

Ahlström, M. A. & Lundqvist, L. (2015). Stand development during 16–57 years in partially harvested sub-alpine uneven-aged Norway spruce stands reconstructed from increment cores. *Forest Ecology and Management*, 350: 81-86. doi: https://doi.org/10.1016/j.foreco.2015.04.021.

Allen, M., Brunner, A., Antón-Fernández, C. & Astrup, R. (2020). The relationship between volume increment and stand density in Norway spruce plantations. *Forestry*, 94 (1): 151-165. doi: https://doi.org/10.1093/forestry/cpaa020.

Andersson, S. (2015). *Tilvekst på bestands- og enkelttrenivå ti år etter selektiv hogst etter KONTUS-prinsippet*. Master's thesis. Ås: Norwegian University of Life Sciences.

Andreassen, K. (1994). *Development and yield in selection forest*. Ås.

Assmann, E. (1970). *The Principles of Forest Yield Study. Studies in the Organic Production, Structure, Increment and Yield of Forest Stands*. Oxford: Pergamon Press.

Aulie, A. (2013). *Vekst og utvikling hos foryngelse etter selektive hogster*: Norwegian University of Life Sciences.

Avery, T. E. & Burkhart, H. E. (2015). *Forest Measurements*. 5th edition ed. Long Grove, IL: Waveland Press Inc.

Bellù, L. G. & Liberati, P. (2006). *Inequality Analysis: The Gini Index*. s.l.

Bianchi, S., Myllymaki, M., Siipilehto, J., Salminen, H., Hynynen, J. & Valkonen, S. (2020). Comparison of Spatially and Nonspatially Explicit Nonlinear Mixed Effects Models for Norway Spruce Individual Tree Growth under Single-Tree Selection. *Forests*, 11 (12): 1338. doi: https://doi.org/10.3390/f11121338.

Bourdier, T., Cordonnier, T., Kunstler, G., Piedallu, C., Lagarrigues, G. & Courbaud, B. (2016). Tree Size Inequality Reduces Forest Productivity: An Analysis Combining Inventory Data for Ten European Species and a Light Competition Model. *PLOS ONE*, 11 (3). doi: https://doi.org/10.1371/journal.pone.0151852.

Brantseg, A. (1967). *Furu sønnafjells. Kubering av stående skog. Funksjoner og tabeller*. Meddelelser fra det Norske skogforsøksvesen. Vollebekk.

Braastad, H. (1967). *Produksjonstabeller for bjørk*. Meddelelser fra det Norske skogforsøksvesen.

Castagneri, D., Nola, P., Cherubini, P. & Motta, R. (2012). Temporal variability of size–growth relationships i a Norway spruce forest: the influences of stand structure, logging, and climate. *Canadian Journal of Forest Research*, 42 (3): 550–560. doi: https://doi.org/10.1139/x2012-007.

Chrimes, D. (2004). *Stand Development and Regeneration Dynamics of Managed Uneven-aged Picea abies Forests in Boreal Sweden*. Doctoral Thesis: Swedish University of Agricultural Sciences.

Chrimes, D. & Nilson, K. (2005). Overstorey density influence on the height of Picea abies regeneration in northern Sweden. *Forestry: An International Journal of Forest Research*, 78 (4): 433–442. doi: https://doi.org/10.1093/forestry/cpi039.

De Liocourt, F. (1898). *De L'Aménagement des sapinieres*. Bulletin trimestriel.

Eerikäinen, K., Valkonen, S. & Saksa, T. (2014). Ingrowth, survival and height growth of small trees in uneven-aged Picea abies stands in southern Finland. *Forest Ecosystems*, 1. doi: https://doi.org/10.1186/2197-5620-1-5.

Forrester, D. I. (2019). Linking forest growth with stand structure: Tree size inequality, tree growth or resource partitioning and the asymmetry of competition. *Forest Ecology and Management*, 447: 139-157. doi: https://doi.org/10.1016/j.foreco.2019.05.053.

Glommen Skogeierforening & Mjøsen Skogeierforening. (2005). *Prosjekt KONTUS Sluttrapport*. Elverum.

Hagner, M. (2015). *Naturkultur: ekonomiskt skogsbruk kännetecknat av befriande gallring och berikande plantering*.

Hanssen, K. H. (2007). *Endringer i mikroklima ved lukkede hogster*. Ås.

Hanssen, K. H., Granhus, A. & Brean, R. (2007). *Vitalitet, avgang og skader på foryngelsen ved selektiv hogst*. Ås.

Helliwell, R. & Wilson, E. (2012). Continuous cover forestry in Britain: challenges and opportunities. *Quarterly Journal of Forestry*, 106 (3): 214-224.

Hynynen, J. (2014). *Learning by doing – Continuous Cover Forestry in Finland* (PowerPoint presentation).

Lei, X., Wang, W. & Peng, C. (2009). Relationships between stand growth and structural diversity in spruce-dominated forests in New Brunswick, Canada. *Canadian Journal of Forest Research*, 39 (10): 1835–1847. doi: https://doi.org/10.1139/X09-089.

Lindhagen, A. & Hörnsten, L. (2000). Forest recreation in 1977 and 1997 in Sweden: changes in public preferences and behaviour. *Forestry: An International Journal of Forest Research*, 73 (2): 143–153. doi: https://doi.org/10.1093/forestry/73.2.143.

Lundqvist, L. (2004). Stand development in uneven-aged sub-alpine Picea abies stands after partial harvest estimated from repeated surveys. *Forestry: An International Journal of Forest Research*, 77 (2): 119–129. doi: https://doi.org/10.1093/forestry/77.2.119.

Lundqvist, L., Chrimes, D., Elfving, B., Mörling, T. & Valinger, E. (2007). Stand development after different thinnings in two uneven-aged Picea abies forests in Sweden. *Forest Ecology and Management*, 238 (1-3): 141-146. doi: https://doi.org/10.1016/j.foreco.2006.10.006.

Lundqvist, L. (2012). *Virkesproduktion och inväxning i skiktad skog efter höggallring*. Jönköping.

Lundqvist, L., Cedergren, J. & Eliasson, L. (2014). *Blädningsbruk*. Skogsskötselserien, 11.
Lundqvist, L. (2017). Tamm Review: Selection system reduces long-term volume growth in Fennoscandic uneven-aged Norway spruce forests. *Forest Ecology and Management*, 391: 362-375. doi: https://doi.org/10.1016/j.foreco.2017.02.011.
Lähde, E., Laiho, O., Norokorpi, Y. & Saksa, T. (1994). Structure and yield of all-sized and even-sized conifer-dominated stands on fertile sites. *Annales des Sciences Forestières*, 51 (2): 97 - 109. doi: https://doi.org/10.1051/forest:19940201.
Lähde, E., Laiho, O., Norokorpi, Y. & Saksa, T. (2002). Development of Norway spruce dominated stands after single-tree selection and low thinning. *Canadian Journal of Forest Research*, 32 (9): 1577–1584. doi: https://doi.org/10.1139/x02-075.
Mäkinen, H., Seo, J., Nöjd, P., Schmitt, U. & Jalkanen, R. (2008). Seasonal dynamics of wood formation: a comparison between pinning, microcoring and dendrometer measurements. *European Journal of Forest Research*, 127: 235–245. doi: https://doi.org/10.1007/s10342-007-0199-x.
Näslund, M. (1942). *Den gamla norrländska granskogens reaktionsförmåga efter genomhuggning*. Stockholm: Statens skogsförsöksanstalt.
Pukkala, T. (2016). Which type of forest management provides most ecosystem services? *Forest Ecosystems*, 3. doi: https://doi.org/10.1186/s40663-016-0068-5.
Savilaakso, S., Johansson, A., Häkkilä, M., Uusitalo, A., Sandgren, T., Mönkkönen, M. & Puttonen, P. (2021). What are the effects of even-aged and uneven-aged forest management on boreal forest biodiversity in Fennoscandia and European Russia? A systematic review. *Environmental Evidence*, 10 (1). doi: https://doi.org/10.1186/s13750-020-00215-7.
Schütz, J.-P. (1975). Dynamique et conditions d'équilibre des peuplements jardinées sur les stations de la hêtraie à sapin. *Schweizerische Zeitschrift für Forstwesen*, 126 (9): 637–671.
Sharma, R. P. & Breidenbach, J. (2015). Modeling height-diameter relationships for Norway spruce, Scots pine, and downy birch using Norwegian national forest inventory data. *Forest Science and Technology*, 11: 44-53. doi: https://doi.org/10.1080/21580103.2014.957354.
Smith, D. M., Larson, B. C., Kelty, M. J. & Ashton, M. S. (1997). *The Practice of Silviculture: Applied Forest Ecology*. 9th edn ed. s.l.: John Wiley & Sons, Inc.
Steinset, T. A. & skogselskap, D. N. (1999). *Norsk skoghåndbok 2000*: Landbruksforlaget
Sterba, H. & Zingg, A. (2001). Target diameter harvesting — a strategy to convert even-aged forests. *Forest Ecology and Management*, 151 (1-3): 95-105. doi: https://doi.org/10.1016/S0378-1127(00)00700-3.
Sterba, H. (2004). Equilibrium Curves and Growth Models to Deal with Forests in Transition to Uneven-Aged Structure – Application in Two Sample Stands. *Silva Fennica*, 38 (4): 413–423. doi: https://doi.org/10.14214/sf.409.
Tveite, B. & Braastad, H. (1981). Bonitering for gran, furu og bjørk. *Norsk skogbruk* (4): 17-22.
Valkonen, S., Lappalainen, S., Lähde, E., Laiho, O. & Saksa, T. (2017). Tree and stand recovery after heavy diameter-limit cutting in Norway spruce stands. *Forest Ecology and Management*, 389: 68-75. doi: https://doi.org/10.1016/j.foreco.2016.12.016.
Valkonen, S., Giacosa, L. A. & Heikkinen, J. (2020). Tree mortality in the dynamics and management of uneven-aged Norway spruce stands in southern Finland. *European Journal of Forest Research*, 139: 989–998. doi: https://doi.org/10.1007/s10342-020-01301-8.
Vestjordet, E. (1967). *Funksjoner og tabeller for kubering av stående gran*. Meddelelser fra det Norske skogforsøksvesen. Vollebekk
West, P. W. (2014). Calculation of a Growth Dominance Statistic for Forest Stands. *Forest Science*, 60 (6): 1021–1023. doi: https://doi.org/10.5849/forsci.13-186.
Woxholtt, S. & Orlund, A. (eds). (2009). *Skogforskningens historie 1967-2006*. Ås: Norsk institutt for skog og landskap.
Zeide, B. (2001). Thinning and Growth: A Full Turnaround. *Journal of Forestry*, 99 (1): 20–25. doi: https://doi.org/10.1093/jof/99.1.20.

Økseter, P. & Myrbakken, S. (2005). *Økonomi og planlegging ved forvaltningsprinsippet KONTUS sammenlignet med flatehogst*, 13. Elverum.

Øyen, B. H. & Nilsen, P. (2002). Growth effects after mountain forest selective cutting in southeast Norway. *Forestry: An International Journal of Forest Research*, 75 (4): 401–410. doi: https://doi.org/10.1093/forestry/75.4.401.

Appendix 1

This appendix contains the tree maps of all plots. Ingrowth in different periods is marked in each plot.

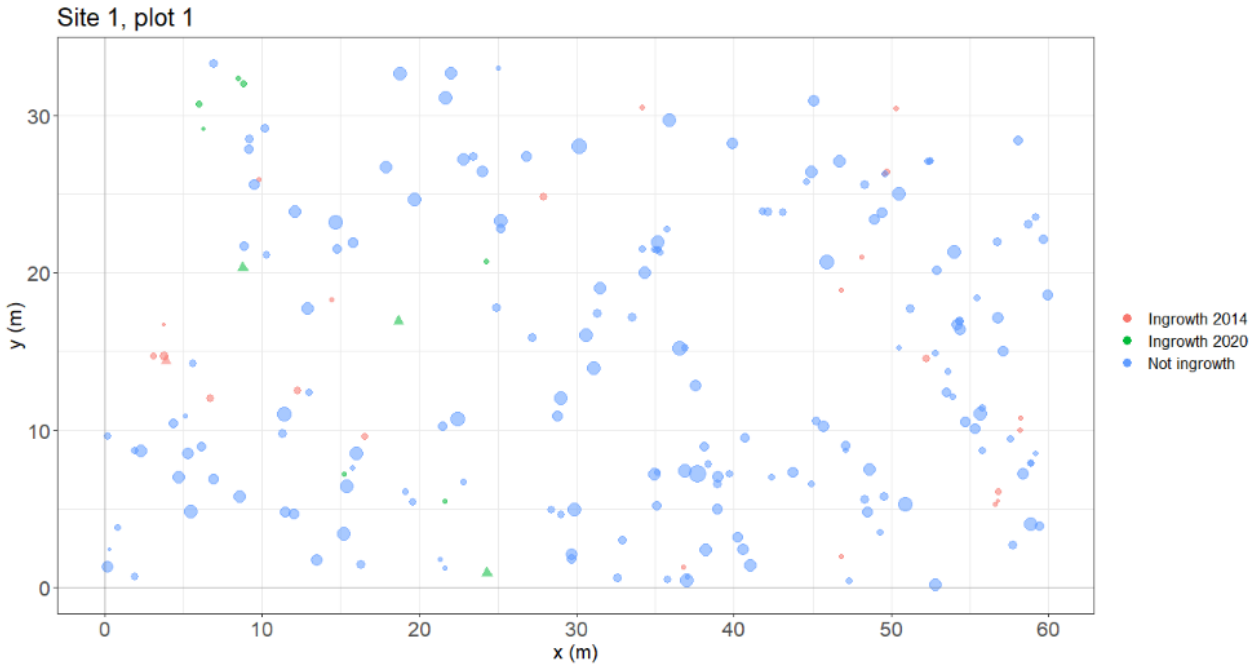

Tree map of site 1, plot 1 in 2020. Planted ingrowth trees are marked with a triangle. Bubble sizes are proportional to DBH.

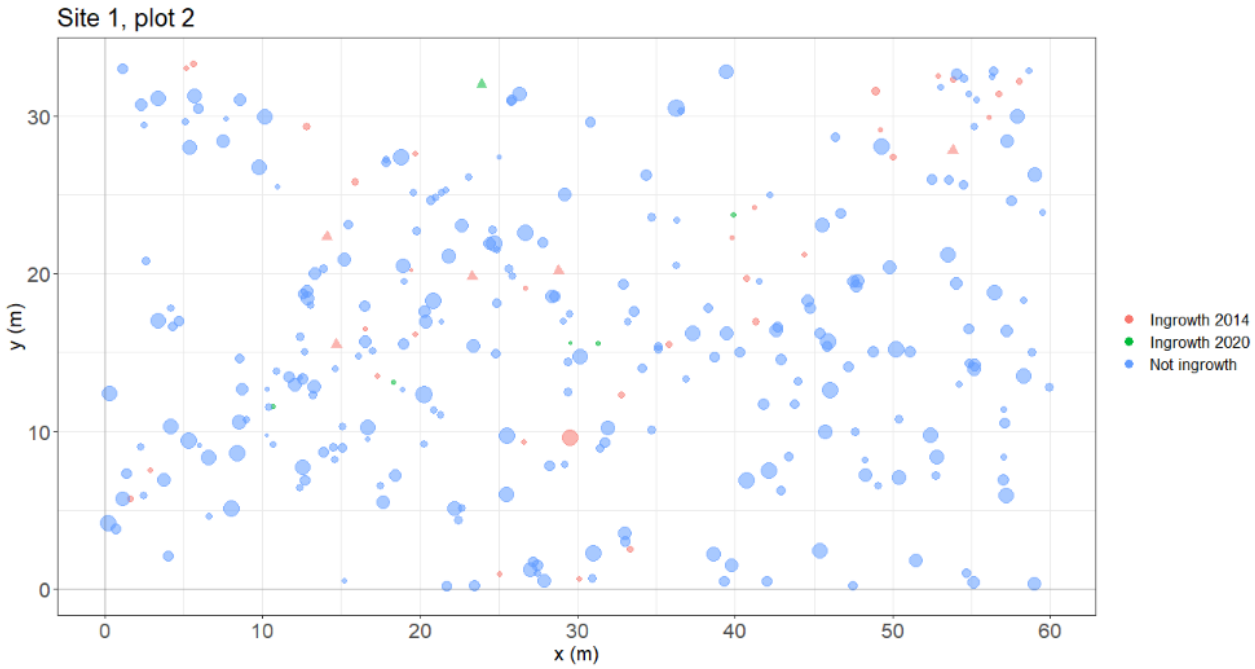

Tree map of Site 1, plot 2 in 2020. Planted ingrowth trees are marked with a triangle. Bubble sizes are proportional to DBH.

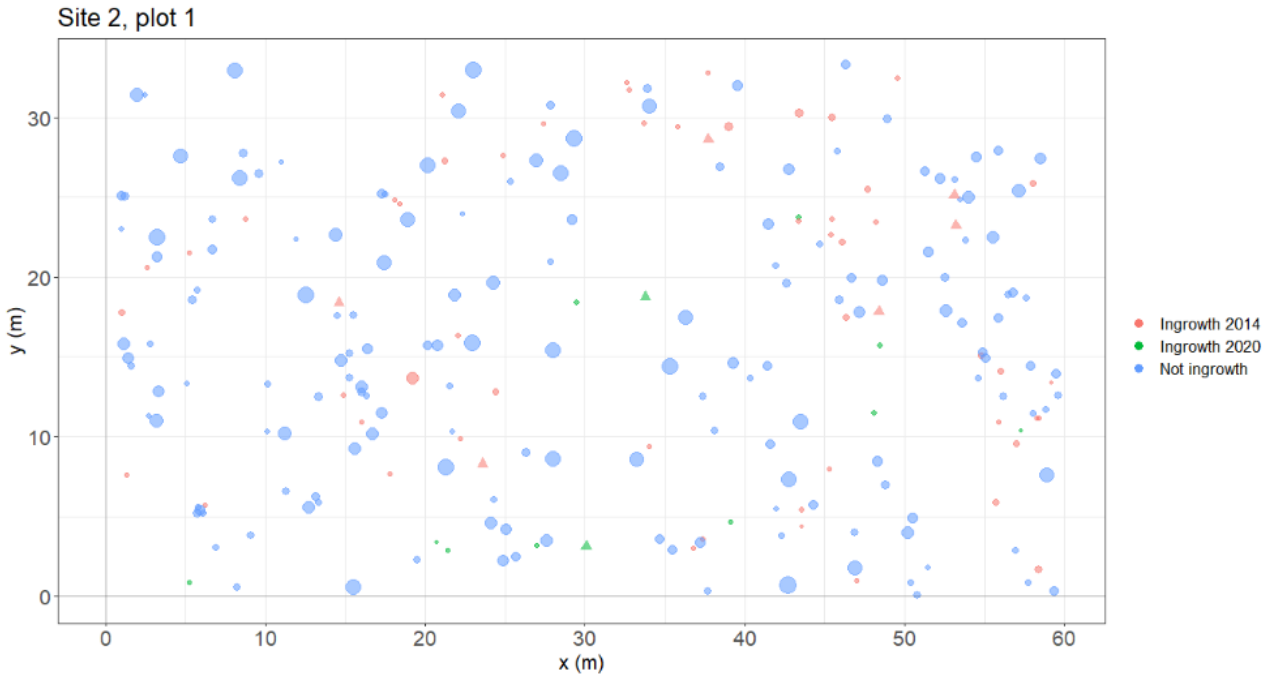

Tree map of Site 2, plot 1 in 2020. Planted ingrowth trees are marked with a triangle. Bubble sizes are proportional to DBH.

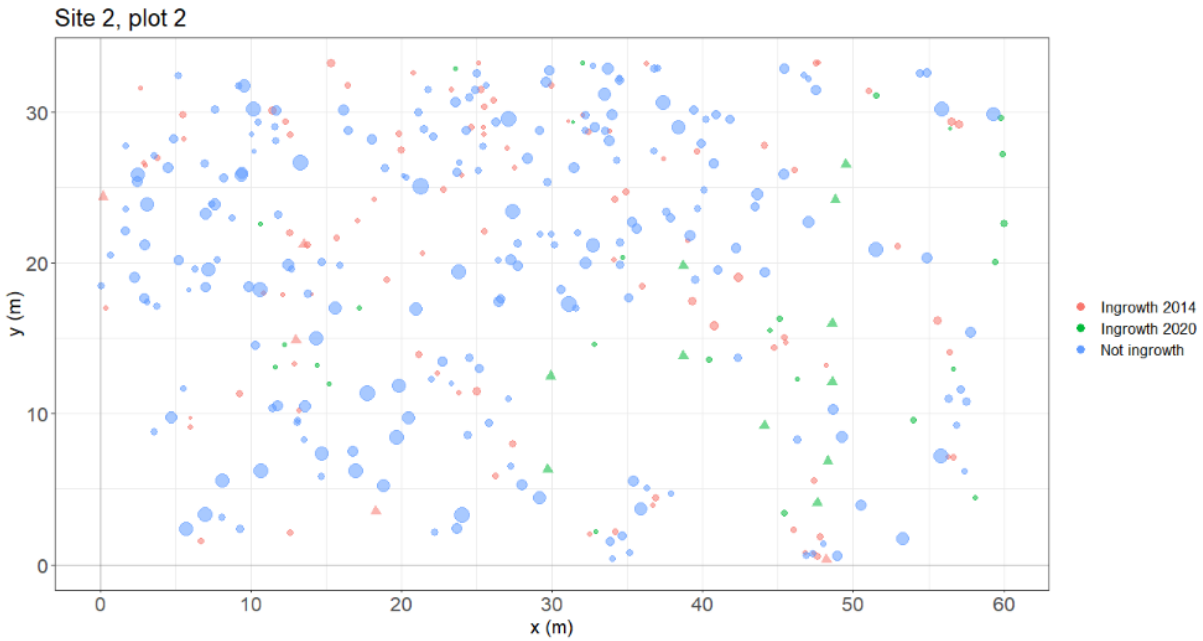

Tree map of Site 2, plot 1 in 2020. Planted ingrowth trees are marked with a triangle. Bubble sizes are proportional to DBH.

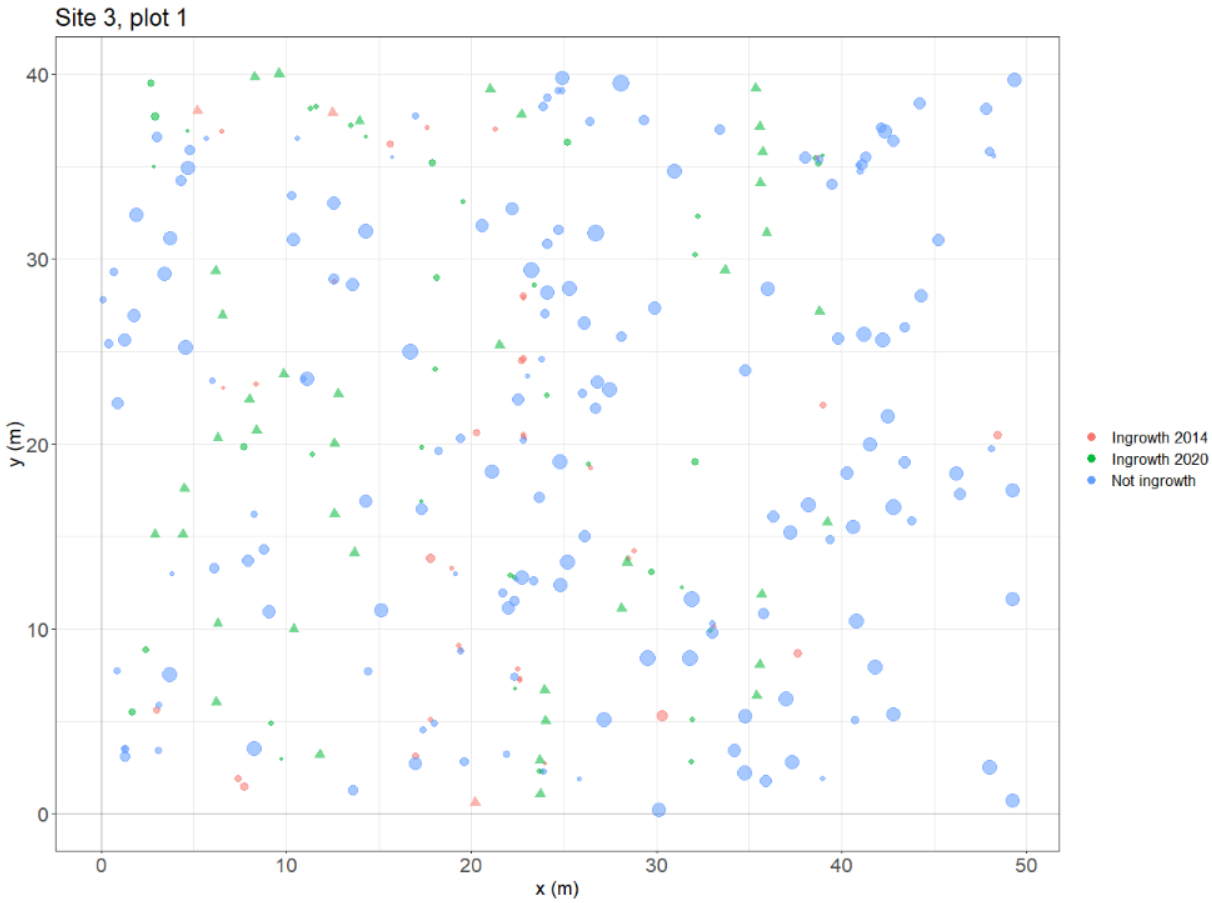

Tree map of Site 3, plot 1 in 2020. Planted ingrowth trees are marked with a triangle. Bubble sizes are proportional to DBH.

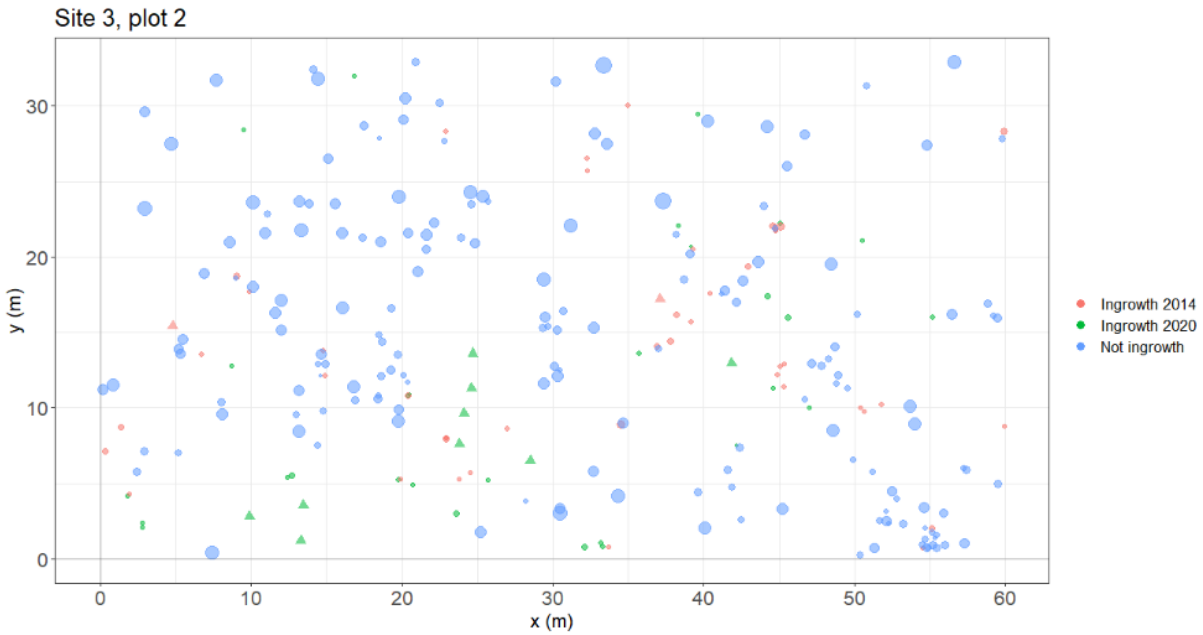

Tree map of Site 3, plot 2 in 2020. Planted ingrowth trees are marked with a triangle. Bubble sizes are proportional to DBH.

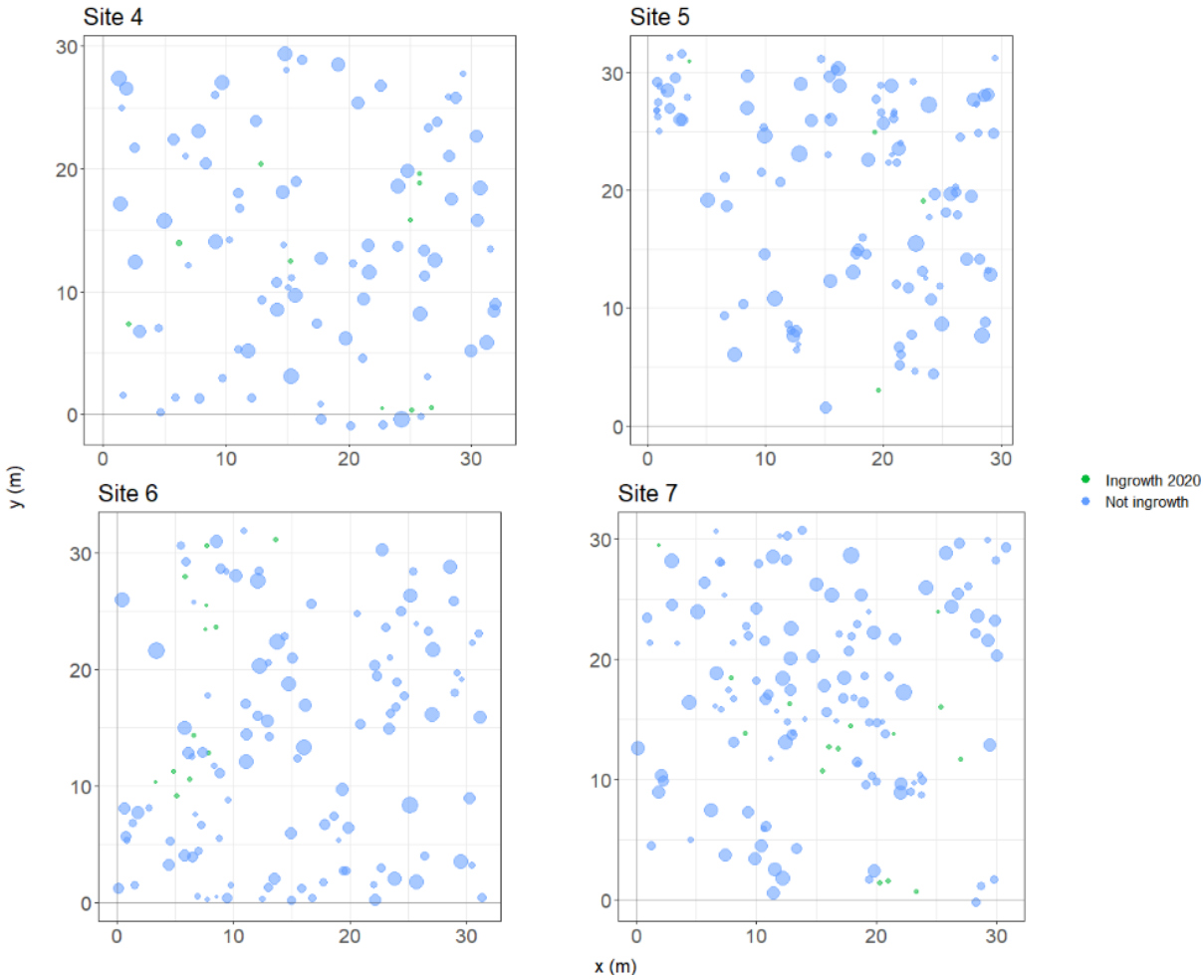

Tree map of Site 4, Site 5, Site 6, and Site 7 in 2020. Bubble sizes are proportional to DBH.

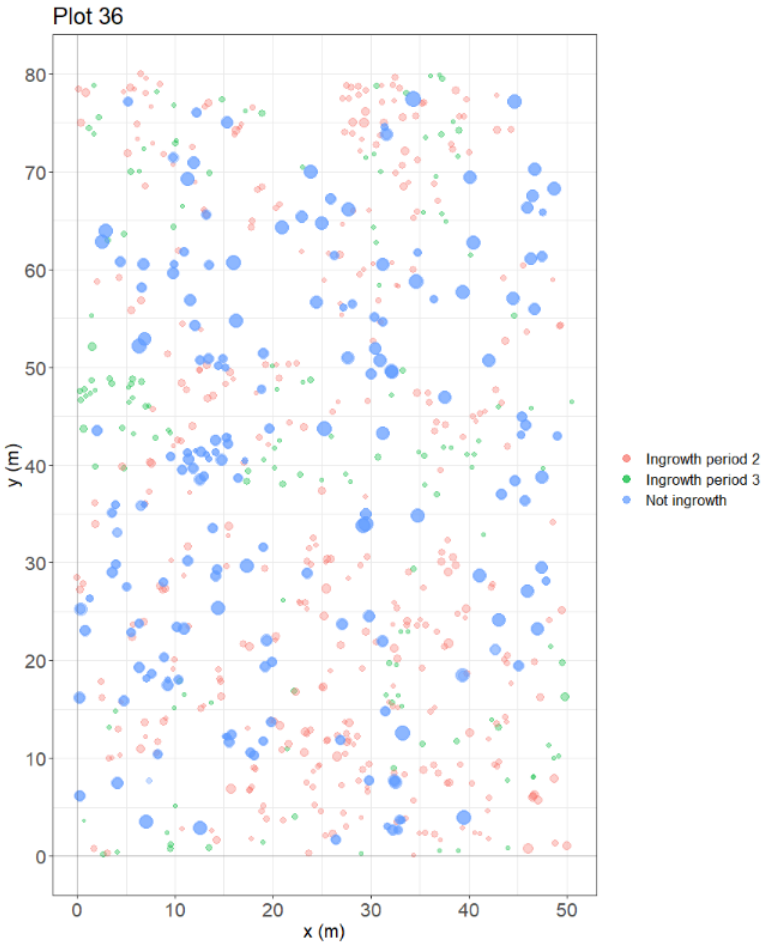

Tree map of plot 36. Bubble sizes are proportional to DBH.

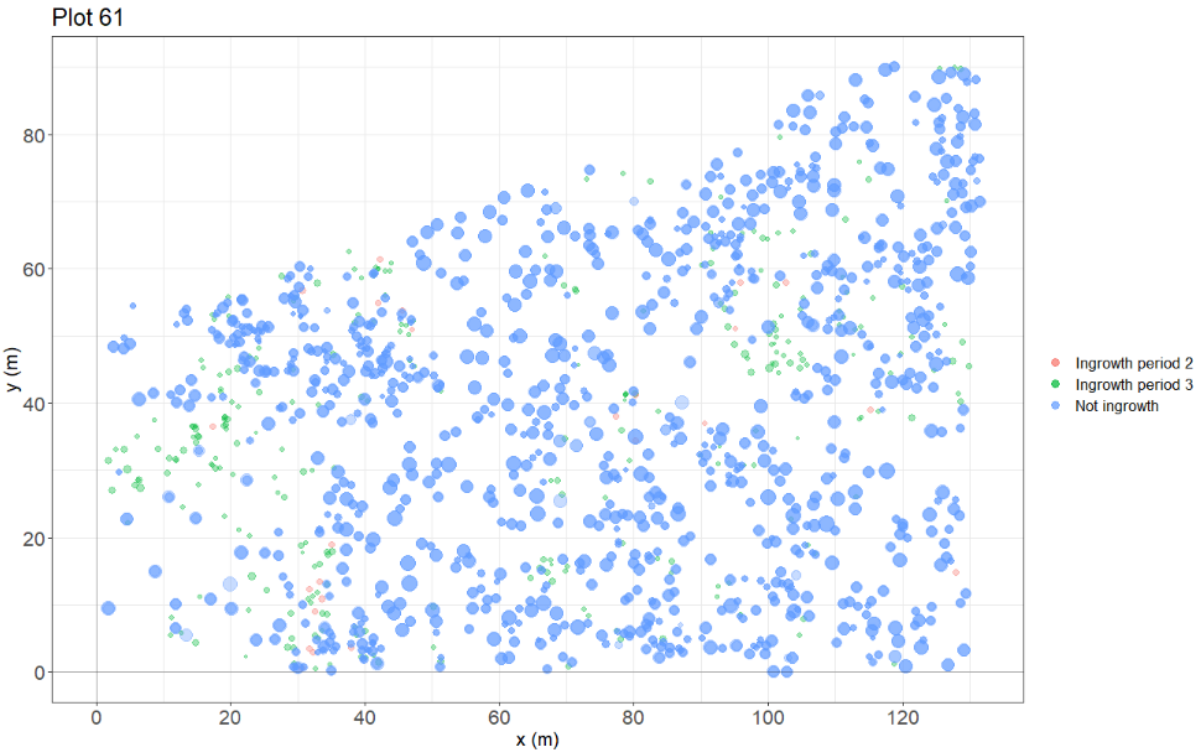

Tree map of plot 61. Bubble sizes are proportional to DBH.

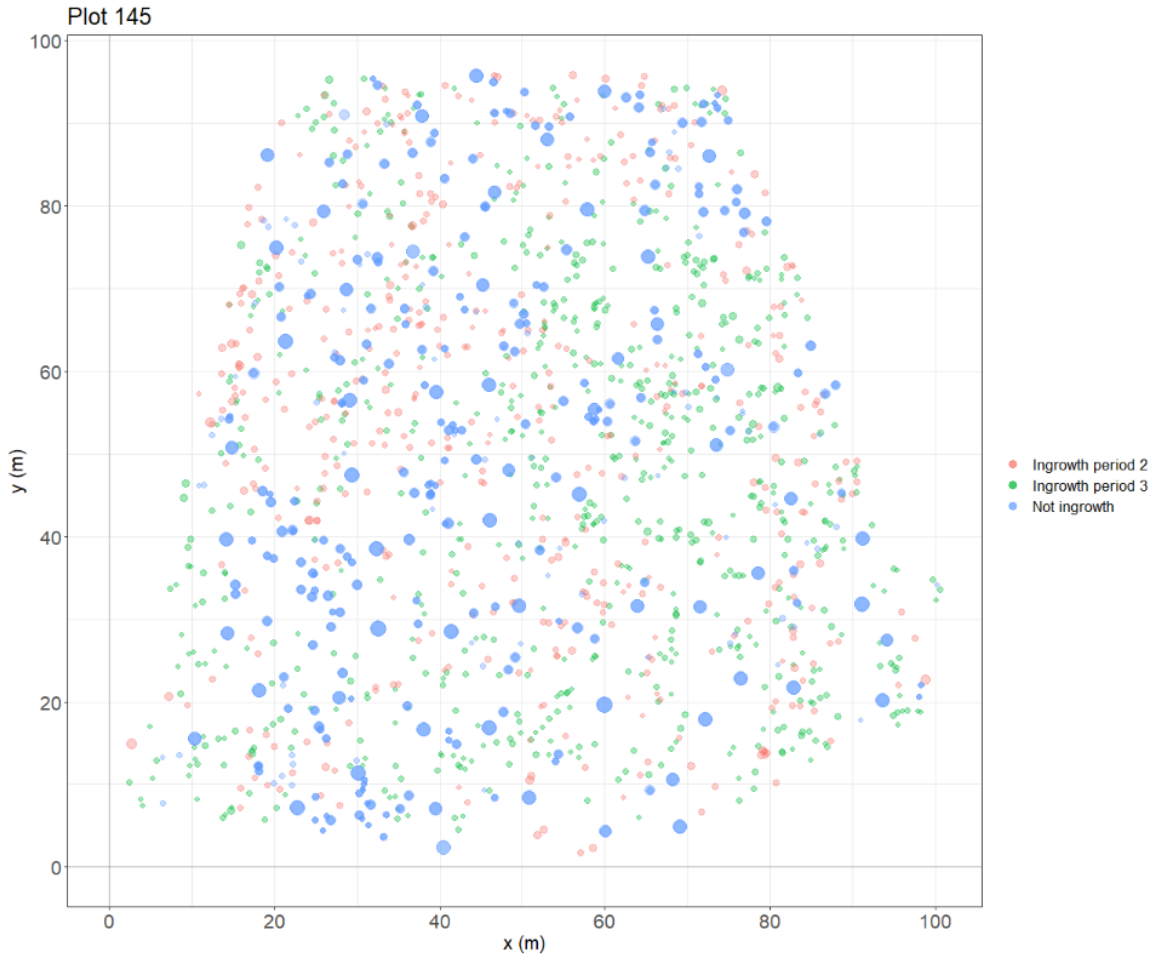

Tree map of plot 145. Bubble sizes are proportional to DBH.

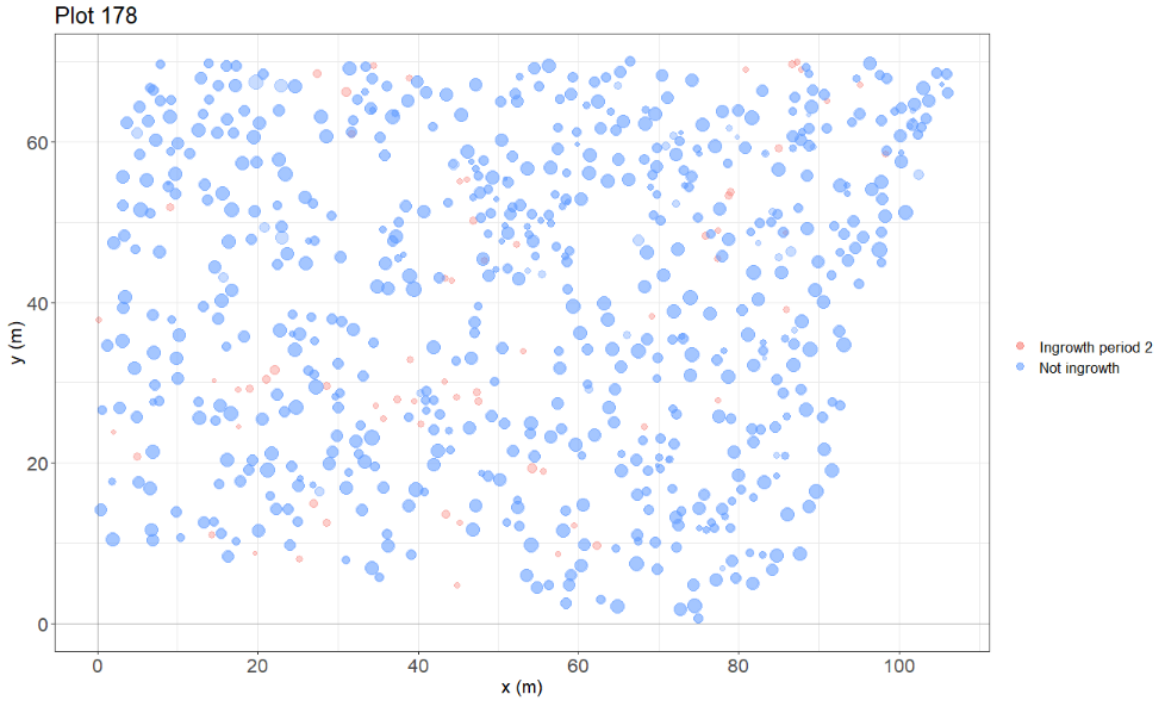

Tree map of plot 178. Bubble sizes are proportional to DBH.

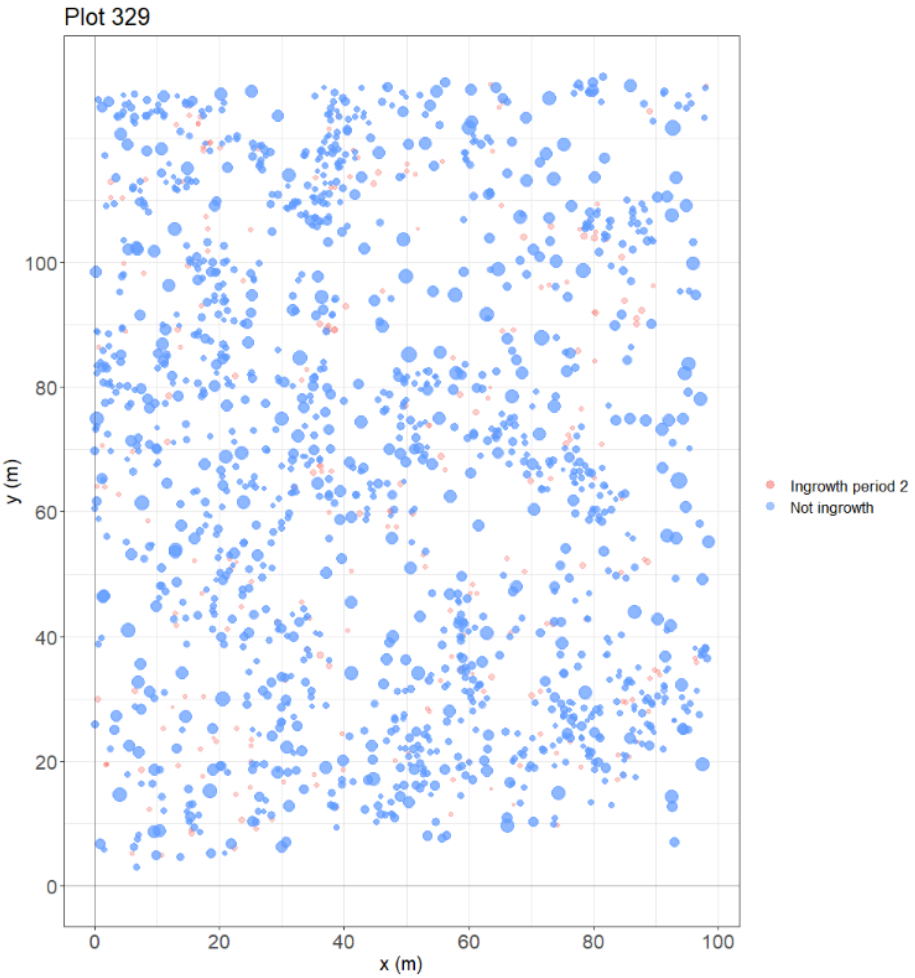

Tree map of plot 329. Bubble sizes are proportional to DBH.

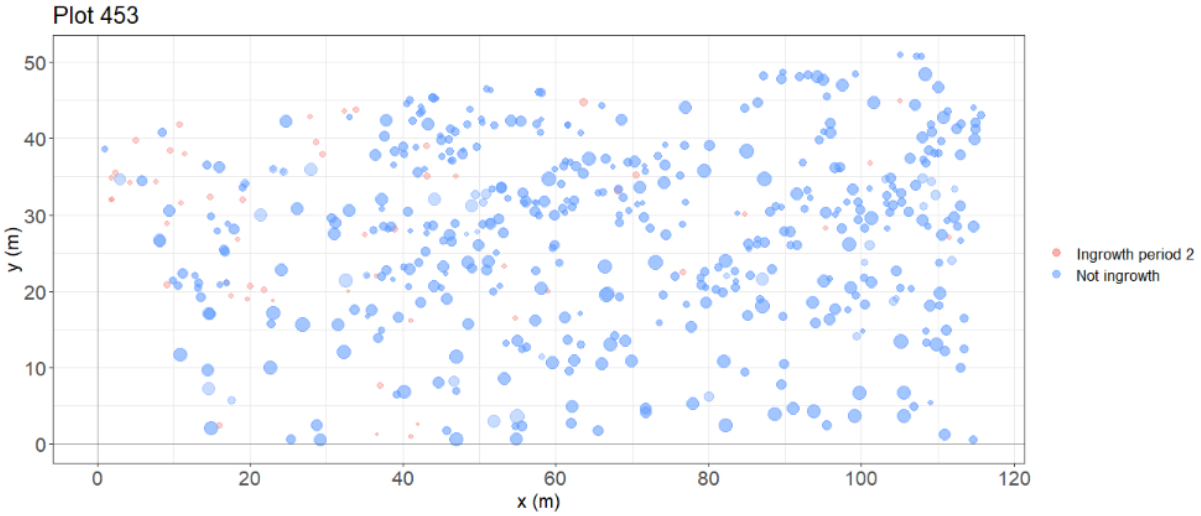

Tree map of plot 453. Bubble sizes are proportional to DBH.

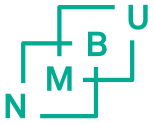

Norges miljø- og biovitenskapelige universitet
Noregs miljø- og biovitskapelege universitet
Norwegian University of Life Sciences

Postboks 5003
NO-1432 Ås
Norway